DEPARTAMENTO DE CIÊNCIAS DA VIDA
FACULDADE DE CIÊNCIAS E TECNOLOGIA
UNIVERSIDADE DE COIMBRA

Mechanisms and possible function of SIRT3 in mESC

Dissertação apresentada à Universidade de Coimbra para cumprimento dos requisitos necessários à obtenção do grau de Mestre em Bioquímica, realizada sob a orientação científica do Professor Doutor João Ramalho-Santos (Universidade de Coimbra).

Marcelo Filipe Maleiro Ribeiro

2015

"We must understand the Cosmos as it is and not confuse how it is with how we wish it to be."
– Carl Sagan, Cosmos

Agradecimentos

Quero agradecer, em primeiro lugar, ao Professor João Ramalho-Santos, por me ter orientado, por me ter aceitado no seu grupo, e por me ter dado condições para que este ano, altamente educativo, tenha sido possível. Quero agradecer-lhe ainda, por me ter, logo no início, chamado à razão sobre a impraticabilidade de alguns projectos, por ter sido directo, e por me ensinar a distinguir entre o que vale ou não a pena.

Agradecer, em segundo lugar, ao meu homónimo, o Marcelo, porque me ensinou tudo o que sei, e a quem devo todas as boas práticas, pensamento crítico, e potencial de organizar o meu trabalho. Agradeço-lhe a paciência, o tempo que dispensou comigo, sem nada pedir em troca. Não há palavras que consigam descrever o quão verdadeiramente lhe estou agradecido, por tudo.

À Inês, companheira de aventuras e de temporadas no laboratório, de momentos de cariz aleatório, por me ter ajudado a tornar fáceis as coisas difíceis, a aprender a dar valor às coisas simples que há no dia-a-dia no laboratório, estou seriamente grato!

Gostava de agradecer também à "malta de stem", e também a todos os restantes elementos do grupo, que além de me terem integrado nos seus quotidianos científicos, também deixaram em mim uma pequena marca de quem são. Mesmo não pertencendo ao grupo, não podia deixar de agradecer à Ana Fernandes, que na sua curta permanência no laboratório, fez-me ver que nunca sabemos tudo sobre nada, por muito que achemos que sim.

Aos professores que possam ou não ter hipótese de ler este agradecimento, deixo também o meu obrigado, porque de um ou outro modo, permitiram que este momento se proporcionasse.

Os meus amigos de sempre, que por escolha própria, pouco vacilando, e sempre voltando, pelos momentos de alento, e por fazerem tão parte de mim como os meses fazem um calendário, deviam agradecer-me, tal como (mas não tanto) eu lhes agradeço a eles! Assim como aos colegas, os mais novos, os mais velhos, os mais antigos e os mais recentes. Mas mesmo no meio destes irmãos e irmãs de armas existem aqueles que se distinguem, agradeço especialmente aos meus "brothers from other mothers".

E por fim, mas nunca menos importante, quero agradecer aos meus familiares, o meu pai, a minha mãe e a minha irmã, pela compreensão, pela paciência, pelo apoio, por tudo o que fizeram, pelo que não fizeram, por tudo o que ainda fazem, e nunca deixarão de fazer.

"Somos o reflexo das pessoas que nos rodeiam."

Obrigado.

Abbreviations

3T3	3 day Transfer, inoculum $3x10^5$ cells
AcLys	Acetylated Lysine
AFP	Alpha-fetoprotein
ATP / ADP	Adenosine Triphosphate; Adenosine Diphosphate
BCA	Bichonic Acid
Bp	Base Pair(s)
BSA	Bovine Serum Albumin
cDNA	Complementary DNA
ddH_2O	Double Distilled Water
DMEM	Dulbecco's Modified Eagle Medium
DNA	Deoxyribonucleic Acid
dsRNA	Double-stranded RNA
E.coli	*Escherichia coli*
EB	Embryoid Body
ECL	Electrochemiluminescence
ESC	Embryonic Stem Cell
ETC	Electron Transport Chain
FBS	Fetal Bovine Serum
H1	Histone 1
HDAC	Histone Deacetylase Class
hESC	Human Embryonic Stem Cell
HIF	Hypoxia-Inducible Factor
hiPSC	Human induced Pluripotent Stem Cells
ICC	Immunocytochemistry
ICM	Inner Cell Mass
KD	Knockdown
KLF-4	Kruppel-like factor 4
KO	Knockout
KODMEM	Knockout DMEM
KSR	Knockout Serum Replacement
LB	Lysogeny Broth
LIF	Leukemia Inhibitory Factor
LTR	Long Tandem Repeat(s)
MEF	Mouse Embryonic Fibroblast
mESC	Mouse Embryonic Stem Cell
MMP	Mitochondrial Membrane Potential
Mn-SOD	Manganese Superoxide Dismutase
mqH_2O	Ultrapure Water
mRNA	Messenger RNA
mtDNA	Mitochondrial DNA
$NADH/NAD^+$	Nicotinamide adenine dinucleotide
NANOG	Nanog homebox (Tír na nÓg, ancient irish for "Land of Eternal Youth")
NIH-3T3	National Institute of Health – 3T3 cells
OCT4	Octamer-binding transcription factor 4
OXPHOS	Oxidative phosphorylation
PAC	Puromycin N-acetyltransferase
PAGE	Poly-Acrylamide Gel Electrophoresis
PBS	Phosphate Saline Buffer
PDH	Pyruvate Dehydrogenase

PDHK	Pyruvate Dehydrogenase Kinase
PFA	Para-formaldehyde
PVDF	Polyvinylidene fluoride
qRT-PCR	Quantitative, Reverse Transcriptase Polymerase Chain Reaction
RNA	Ribonucleic Acid
ROS	Reactive Oxygen Species
rRNA	Ribosomal RNA
Scr	Scramble/Scrambled
SDS	Sodium Dodecyl Sulfate
shRNA	Short hairpin RNA
siRNA	Small interference RNA
SIRT	Sirtuin, Sir-two homologue protein
SOC	Super Optimum broth with catabolite repression
Sox2	Sex determining region Y – box 2
SRB	Sulforhodamine B
SSEA	Stage specific embryonic antigen
SV40	Simian vacuolating virus 40
TBS-T	Tris-buffered Saline with Tween
TOM20	Translocase of outer mitochondrial membrane 20 homolog
WB	Western Blot
WT	Wild Type
αSMA	Alpha-Smooth Muscle Actin

Resumo

Isoladas do pluriblasto do blastocisto de murganho, as células estaminais embrionárias, com a sua capacidade de auto-renovação e de diferenciação em todos os tecidos adultos, providenciam simultaneamente um excelente modelo de estudo das fases iniciais do desenvolvimento embrionário, com um potencial papel no campo da medicina regenerativa. Longe de compreender todos os mecanismos que governam a regulação da pluripotência e da diferenciação destas células pluripotentes, o metabolismo tem emergido como uma ferramenta para modular estes intricados processos de desenvolvimento celular. O paradigma actual em investigação em células estaminais é de que, durante a diferenciação, alterações metabólicas precedem alterações ao nível genético. Por outro lado, o controlo da actividade de enzimas relevantes para o metabolismo pode trazer também controlo da pluripotência de mESC.

A sirtuína 3, principal deacetilase mitocondrial, tem como alvos enzimas do ciclo de Krebs, a cadeia transportadora de electrões, e da sua actividade advém um aumento da actividade dessas enzimas. É, por isso, associada á activação do metabolismo mitocondrial. Por esse motivo, seria interessante saber se a SIRT3 possui um papel na regulação da pluripotência e/ou diferenciação de mESC.

O silenciamento da expressão de uma proteína providencia um modo de avaliar a importância dessa mesma proteína numa rede de sinalização ou numa via metabólica. Enquanto knockouts genéticos são algo difícil de obter, um knockdown de um gene é relativamente mais fácil de conseguir, enquanto se mantém uma especificidade de alvo que não é conseguida pelo uso de inibição farmacológica. Estes sistemas de knockdown baseiam-se na tecnologia de interferência por RNA, um processo que inibe a expressão de uma proteína ao nível do transcriptoma. Para conseguir este silenciamento, introduzimos um siRNA, tendo como alvo a sequência de mRNA da proteína de interesse.

Deste modo, pretendemos realizar o silenciamento da SIRT3, em mESC, através do uso de um shRNA que tem como alvo o mRNA da SIRT3. Como o propósito deste ensaio é realizar um silenciamento estável, utilizámos um plasmídeo que expressa o supracitado shRNA, incorporado pelas células estaminais por lipofecção. Assim, neste trabalho, pretendeu-se estabelecer um protocolo de silenciamento de uma proteína, com recurso à transfecção de um plasmídeo que expressa um shRNA que tem como alvo a SIRT3.

Os resultados mostram que a transfecção de mESC não é tão simples e directa como previsto, e não pudemos obter uma cultura principalmente composta por células E14Tg2.a transfectadas. No entanto, conseguimos transfectar fibroblastos embriónicos de murganho (NIH-3T3) e ainda obtivemos uma cultura enriquecida em células transfectadas. Apesar disto, o silenciamento de SIRT3 não foi claro, e portanto, a avaliação deste silenciamento deve ser repetida.

Palavras-chave: Células estaminais embrionárias de murganho; metabolismo; Sirtuína3; interferência de RNA; Lipofecção.

Abstract

First derived from the inner cell mass of the mouse blastocyst, Embryonic Stem Cells, with their capability of self-renewal and of differentiation in all adult tissues, simultaneously provide an excellent model for studying early development and can play a role in regenerative medicine. Far from understanding all the mechanisms that rule the regulation of pluripotency and differentiation of these pluripotent cells, metabolism has emerged as a tool to modulate these intricate cell development processes. The current paradigm in stem cell research is that, during differentiation, metabolic alterations precede changes in gene expression, and also, that through the control of the activity of certain, metabolically relevant enzymes, one can modify the "stemness" of mESC.

SIRT3, regarded as the main mitochondrial deacetylase, targets metabolic enzymes belonging to the Krebs' Cycle and also the Electron Transport Chain, and its deacetylating activity promotes the activity of these enzymes. It is then associated with the activation of the mitochondrial metabolism. Therefore, we took interest in whether there is role of SIRT3 in the regulation of pluripotency and differentiation of mESC.

Protein silencing provides a means of assaying the importance of a given protein to signaling network or a metabolic pathway. While specific genetic knockouts are rather difficult to obtain, a gene knockdown is relatively easier to obtain while maintaining a specificity degree that can't be achieved through pharmacological inhibition. These knockdown systems are often based on RNA interference, a process by which the cell inhibits gene expression on the transcriptome level.

Here, we expected to silence the expression of SIRT3 in mESC by using a SIRT3 mRNA-targeting shRNA. As we aim for a relatively stable protein knockdown, we used shRNA expressing plasmids that were incorporated in mESC by Lipofection (a form of transfection). Thus, in this work, we aimed to establish a protein silencing protocol, with a SIRT3 shRNA-encoding plasmid, previously transfected into the targeted cells.

Results show that mESC are not as easy to transfect and select as previously reported, as we were not able to obtain a culture majorly composed of transfected E14Tg2.a cells. Nonetheless, we successfully transfected mouse embryonic fibroblasts (NIH-3T3), and obtained an enriched culture in transfected cells. Even so, the SIRT3 silencing rate was not clear, and further evaluation of this silencing should be performed.

Keywords: mouse Embryonic Stem Cells; metabolism; Sirtuin3; RNA interference; Lipofection

TABLE OF CONTENTS

1 INTRODUCTION

1.1 MESC

1.1.1 Historical context

Embryonic Stem Cells (ESCs) are derived from the inner cell mass (ICM) of the blastocyst and were first identified in 1981 by Martin Evans, Matthew Kaufman (Evans and Kaufman, 1981) and Gail R. Martin (Martin, 1981), from mouse embryos.

As seen in Figure 1, ESCs have two main features: the ability to continuously self-renew (maintaining their pools by symmetric division) and the capacity to differentiate into cells from the three germ lineages (endo, meso and ecotderm). During this process cells change size, shape, and responsiveness to outer and internal signaling, and alter gene expression, in order to perform specific biological roles.

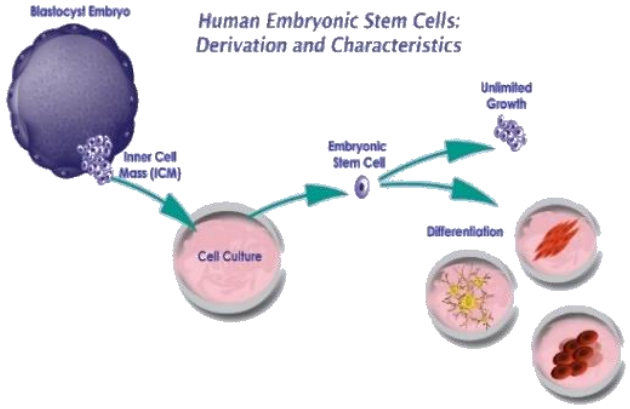

Figure 1 – Derivation of embryonic stem cells (ESCs) from the ICM of the Blastocyst, and schematic differentiation and self-renewal capabilities. Image acquired from https://www.umassmed.edu/iscr/stemcellfacts.aspx, accessed in 28/07/2014)

Firstly appeared to describe an evolutionary, "family"-like relationship by using a phylogenetic tree, the term "stem cell" was coined in the late 19th century by the German biologist Ernst Haeckel (Haeckel, 1879), who employed the term "stembäume" for these phylogenetic trees – family trees, or stem trees, as was adapted to English. Thus, he chose the term "stammzelle'', German for Stem cell, to address an unicellular organism ancestor from all the other organisms originated. Later, in 1892, Theodor Boveri used the term stem cell with the same "family lineage" purpose in mind (Ramalho-Santos and Willenbring, 2007). Again, in the beginning of the 20th century, the term was once more used by Alexander Maximow, in his Unitarian theory of Hematopoiesis (Maximow, 2009), where the stem cells were described to be the undifferentiated hematopoietic progenitors, that were "neither red nor white blood corpuscles". But only during the 1960's the term resurfaced, when proof of adult neurogenesis in the brain pointed to the existence of stem cells (Altman and Das, 1967). In the late 1970's

it was established that stem cells were capable to support bone marrow transplants, a practice that is commonly employed today (Peister et al., 2004).

1.1.2 Characterization of mouse ESC (mESC)

Along with their ability to generate all three germ layers, ESCs are characterized by the increased expression of "core pluripotency markers": Oct4, Sox2 and Nanog (Hanna et al., 2010). These factors form a hierarchical pluripotency core network signaling that converges towards activation of self-renewal and pluripotency through Oct4, while exhibiting a strong self-regulation mechanism (Kim et al., 2008). As cells differentiate there is a loss of this network signaling and the levels of the aforementioned factors decreases over time. This is common to both human ESC (hESC) and mESC. This network can be stimulated exogenously, in order to maintain pluripotency of these cells while in culture. Leukemia inhibitory factor (LIF, an interleukin 6-class cytokine) is reported to keep the pluripotent phenotype of mESC mainly through activation of the Jak2/Stat3 signaling pathway, which culminates in an increased expression of Oct4. Nonetheless, LIF acts through other pathways culminating with the same effect. Figure 2 shows two alternative pathways by which LIF regulates pluripotency: 1) through PI(3)K-Akt axis, increasing the expression of Tbx3 which will, in turn, strengthen the expression of the pluripotency core factors (Storm et al., 2007); and 2) also through mitogen-activated protein kinase (MAPK). Incidentally, LIF-mediated activation of MAPK culminates in the inhibition of Tbx3 expression and thus, weakening pluripotency (Ying et al., 2008). Other works supporting this notion have demonstrated that inhibition of MAPK increases pluripotency of mESC (Wray et al., 2011). Alkaline phosphatase staining is regarded as a simple assay to access pluripotency, as ESCs express high levels of this enzyme, constituting therefore as another marker for pluripotency (Singh et al., 2012), that can be easily performed routinely to evaluate pluripotency in culture. Other surface markers for mESC include E-cadherin, CD 133 (prominin-1), Integrin β-1; Epithelial cell adhesion molecule (EpCAM), and stage-specific embryonic antigen (SSEA) 3. (Zhao et al., 2012).

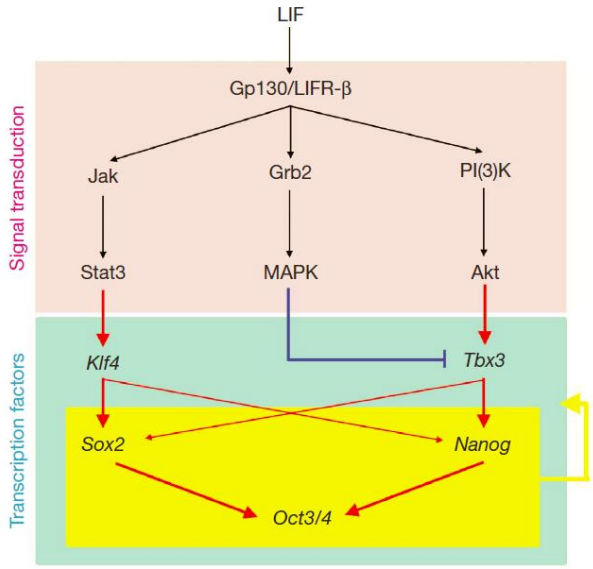

Figure 2 - LIF signals through both Jak/Stat and Akt pathways to stimulate the core pluripotency network and assure the pluripotent phenotype and self-renewal, in mESC.(Niwa et al., 2009)

mESCs are morphologically distinguishable from their differentiated counterparts. Cultured pluripotent colonies are characterized by their round and compact morphology, growing not only in width but also in height; high optical refringence (brilliant, white borders); and a high nucleus/cytoplasm volume ratio. As these colonies start the differentiation process and lose their pluripotent phenotype, cells tend to spread away from the center of the colony, increasing their size (cells can be visually distinguished with the proper magnification), and decreasing refringence. An example of two very different mESC cultures can be seen in Figure 3. Figure 3A shows colonies with good size and morphology, and are ready to be passaged. In Figure 3B, although the pluripotent phenotype is still perceivable in some of the colonies, most of the colonies begun the differentiation process. Strict monitoring of the culture's pluripotent state is essential for its maintenance in culture, as well as confluence (higher or very low confluences may impact pluripotency).

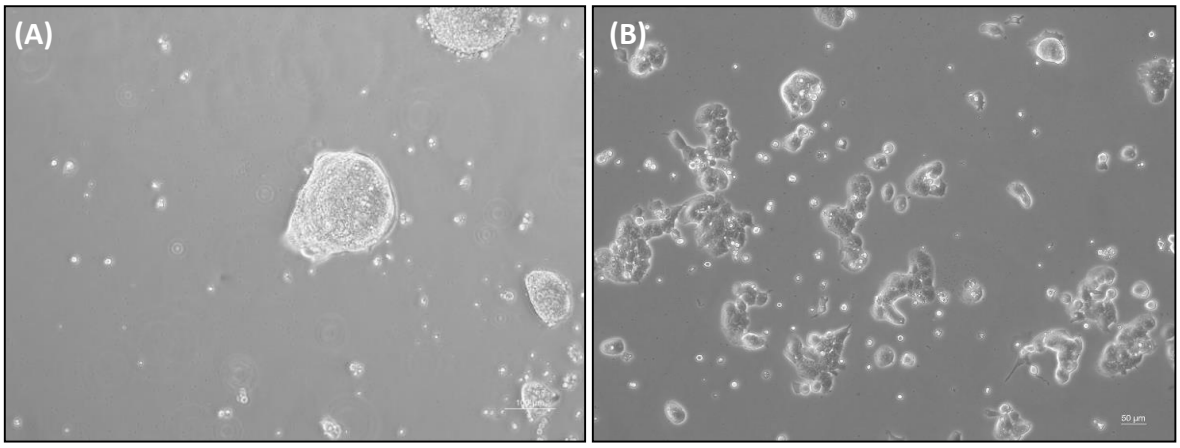

Figure 3 - Pluripotent E14 mESC culture in KODMEM medium. (A) – E14 culture, at day 3, with good morphology; (B) E14 culture at day 3 with poor pluripotent morphology.

In ESCs, the mitochondrial DNA (mtDNA) copy number is low, which is a reflex of a low mitochondrial mass (Baharvand and Matthaei, 2003). Moreover, in these cells mitochondria are small, round, have few cristae in the inner mitochondrial membrane and have a perinuclear localization and low activity of the Electron Transport Chain (ETC) (Facucho-Oliveira and St John, 2009; Ramalho-Santos et al., 2009). Once ESC differentiate, the mitochondria start to disperse throughout the cytoplasm away from the nucleus (as can be clearly seen in Figure 4), increasing in mass, cristae complexity and mtDNA, and start a mitochondrial network that leads to metabolically active mitochondria (Facucho-Oliveira et al., 2007). The expression of ETC complexes also increases, along with their activity, with a characteristic higher mitochondrial membrane potential (MMP) (Schieke et al., 2008). Antioxidant defense-associated enzymes such as manganese superoxide dismutase (Mn-SOD) have their expression increased, in order to counter the now-present reactive oxygen species (ROS) generated from the more-oxidative metabolism (Facucho-Oliveira and St John, 2009).

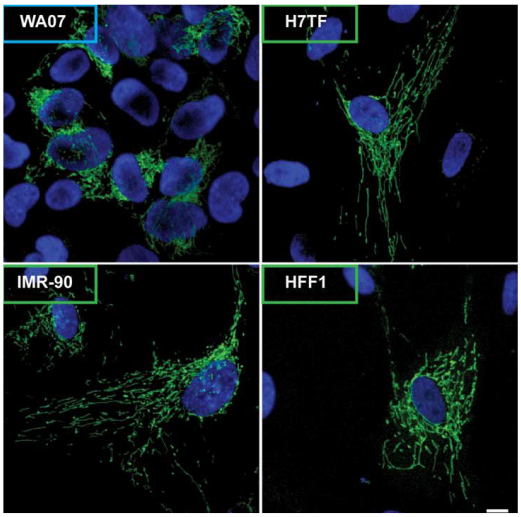

Figure 4 - Mitochondrial morphology and localization, relatively to the nucleus, in WA07 cells (hESCs) and differentiated cells (H7TF, HFF, and IMR-90 lines). Blue (DAPI) is a fluorescent stain that binds to DNA. Green corresponds to GFP-tagged pyruvate dehydrogenase (coded via baculovirus system) (Varum et al., 2011).

1.1.3 Potential uses of stem cells

The current use of Stem Cells in research falls fundamentally at developmental investigation and tissue regeneration. Every medical, pathological situation where cell replacement (due to injury, disease, or other causes) is required, stem cell use may be the key. Type I diabetes, Spinal cord injury, Parkinson's disease, retinal diseases, myocardial infarction, amyotrophic lateral sclerosis, deafness, baldness, blindness, wound healing, are all eligible for stem cell application (Barberi et al., 2003). Hematopoietic stem cells have been used since the 1980's in therapy given that blood marrow transplantation is but a transplantation of hematopoietic stem cells (Bianco et al., 2001; Lin et al., 2013). Stem cells are also a promising tool in toxicological investigation and disease modeling (Lin et al., 2013; Sousa et al., 2013).

Another field where stem cells are involved is cancer research: stem cells, in their pluripotent state, resemble carcinogenic cells in terms of their metabolism, growth rate, migration and signaling pathways. Many scientific aspects, described decades ago and that apply to cancer cells, also apply for stem cells(Martin, 1981). The term "Warburg effect", which addressed the metabolism of cancer cells, coined in 1956, is being now applied for both cancer and ESC alike (Upadhyay et al., 2013; Warburg, 1956). So, whatever we may be able to learn from one field, *may* be transposed to the other.

1.1.4 Metabolism: Warburg-like effect & Metabolic Shift

Along with self-renewal and pluripotency, ESCs should be also noted by their characteristic metabolism. ESCs use glycolysis as their primary source of energy and biosynthetic building blocks, in contrast with differentiated cells, who rely more on the Krebs' Cycle and Oxidative Phosphorylation (OXPHOS) for the same purpose (Pereira et al., 2014). Each pathway requires different enzymatic machinery. Krebs' Cycle shows increased energetic efficiency, complexity, need for oxygen availability, but decreased kinetics. Due to the elevated proliferation and hypoxic niche location in the ICM, *in vivo*, ESCs require a high demand of energy and biomolecules (that should be quickly available) in order to support their proliferation, and thus, ESCs favor glycolysis over oxidative metabolism (Stanley et al., 2013). The Warburg effect, first described by Otto Heinrich Warburg in 1956, reflects the high aerobic glycolysis by malignant tumors even in the presence of oxygen, and this Warburg-like effect in ESCs disappears over the course of differentiation, suggesting that a metabolic shift occurs somewhere along the process. This metabolic shift, requires a reshaping in many cellular aspects, such as mitochondrial morphology and subsequent activity, gene expression, antioxidant defenses, and metabolic reprograming (by activation of mitochondrial metabolism, namely Krebs' Cycle, OXPHOS and the intermediary metabolism (displayed in Figure 5) (Pereira et al., 2014)) precedes alteration of genomic expression (Chen et al., 2012; Cho et al., 2006; Folmes et al., 2011a, 2012; Varum et al., 2011). Recent studies revealed that stem cell metabolism might be a tool for comprehension and fine tuning of differentiation (Chen et al., 2012; Chung and Dzeja, 2007; Folmes et al., 2011a, 2012, 2011b; Grayson and Zhao, 2006; Pattappa et al., 2011; Pereira et al., 2013, 2014; Rafalski et al., 2012; Ramalho-Santos et al., 2009; Robinson et al., 1997; Signer and Morrison, 2013; Simsek et al., 2010; Sousa et al., 2013; Suda et al., 2011; Varum et al., 2011; Weisbart and Kwan, 1987; Yanes et al., 2010; Yoshida et al., 2009). By controlling the metabolic conditions of the medium, such as oxygen availability, forcing the expression of certain genes, such as HIF1-α (Mathieu et al., 2014), or even by inhibiting enzymes that are crucial for key metabolic pathways, stem cell pluripotency /differentiation might be modulated. It has been shown by our group that inhibition of normal mitochondrial metabolism (namely through inhibition of Complex III of the ETC) can block mESC neuronal differentiation (Pereira et al., 2013). Moreover, blocking Complex III of the ETC can enhance the pluripotent phenotype in hESC (Varum et al., 2009). Also, inhibiting PDHK (and thus increasing PDH activity) would favor differentiation in mESC

(Rodrigues et al., 2015). Regulation of both human and mouse ESCs metabolism seems to be linked to their pluripotency and differentiation capacities.

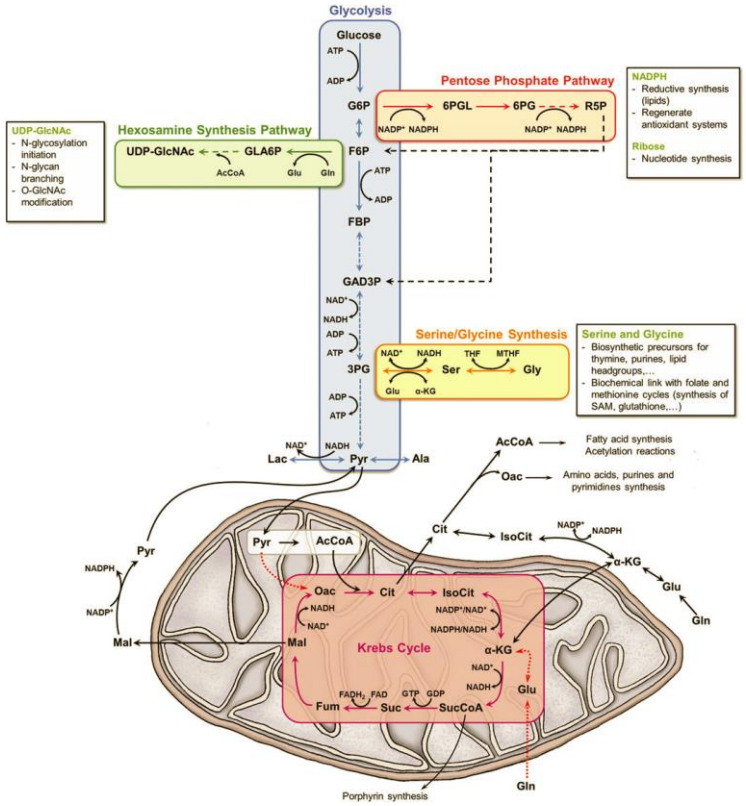

Figure 5 - Primary pathways of glucose metabolism. Both glycolysis, Krebs' cycle, the pentose-phosphate pathway (PPP) and biosynthetic mechanisms are presented. (Pereira et al., 2014)

1.2 Modulation of Metabolism and Pluripotency

The metabolic remodeling that mESC undergo when they differentiate implicate two distinct metabolic profiles. This point is summarized in Figure 6. In this section, I will show evidence of metabolic changes during differentiation, and just how this process may even precede changes in genetic expression.

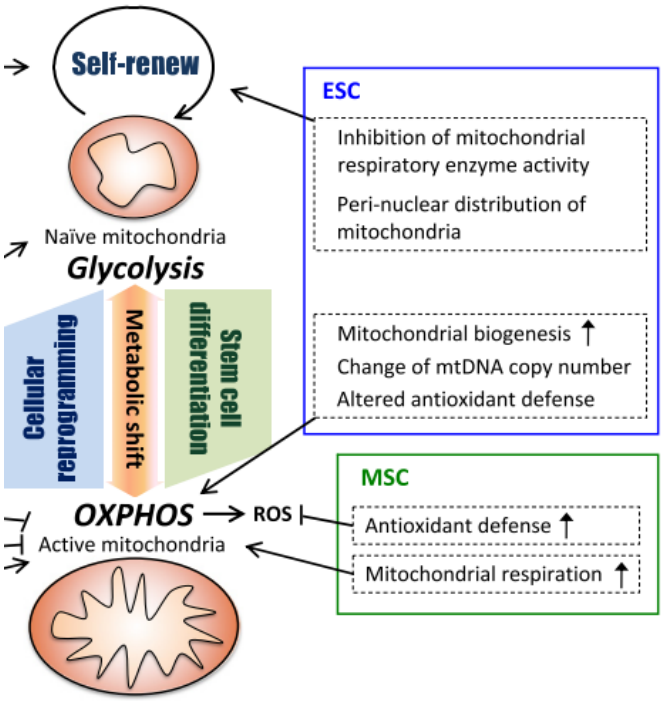

Figure 6 - The metabolic regulation and mitochondrial changes in the maintenance of self-renewal capability and induction of differentiation of different types of stem cells. Adapted from Chen et al. 2012.

There are different metabolic statuses in mESCs, and differentiated cells (MEFs) have been reported, summarized in Figure 6. In order to assay their metabolic profile, lactate and acetate production (by-products of the glycolytic pathway) was measured, as well as the energetic ratio of ADP/ATP, and values of oxygen consumption (which determine the degree of oxidative metabolism), demonstrating that mouse iPSC and mESC show higher concentrations of these metabolites than their more differentiated counterparts, MEFs (Folmes et al., 2011b). Other works saw similar results regarding hESC and hiPSC vs somatic cells (Varum et al., 2011).

Knowing that the metabolic profile is different for each type of cell, and that the aerobic metabolism requires mitochondrial activity, this analysis of the mitochondrial membrane potential of ESC vs MEFs concludes that stem and stem-like cells present higher values of MMP, while differentiated MEFs showed low MMP, as visible in Figure 7, reflecting changes towards a mature and metabolically active organelle (Schieke et al., 2008).

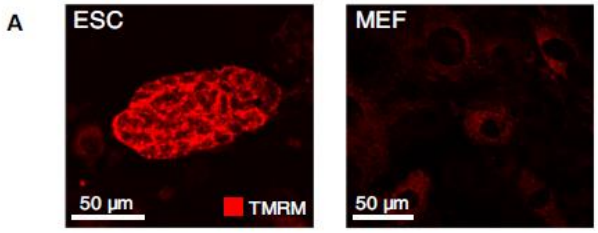

Figure 7 - Live mitochondrial membrane potential (MMP) obtained via TMRM fluorescence. (Folmes et al. 2011)

Further characterization of this change in metabolism, focusing in genetic adaptations, revealed that expression of glycolytic enzymes precedes the expression of pluripotency markers, leading to the conclusion that metabolic adaptations occur before the cell can change its potency degree (Folmes et al., 2012). Again, this pattern was also verified in comparison studies in hESC/iPSCs and differentiated cells (Varum et al., 2011).

1.3 SIRTUINS

Sir-two homologue proteins – Sirtuins (SIRT) are NAD^+-dependent lysine deacetylases. Homologues to Sir-two (first described in yeast), they are considered part of the Histone Deacetylase (HDAC) class I family. Although Sirtuins possess the ability to deacetylate histones, that does not seem to be their only role (Imai et al., 2000). There are seven known mammalian Sirtuins, with varying roles and sub-cellular localizations. Sirtuins 6 and 7 are present in the nucleus, while Sirtuin 1 and 2 allocate both in the cytoplasm and nucleus alike. The last three Sirtuins (3, 4 and 5) take residence in the mitochondrion (Finkel et al., 2009; Haigis and Guarente, 2006).

Apart from Sirtuins 6 and 4 (which have the activity of ADP-ribosyl-transferase), the primary role of sirtuins is deacetylation, the removal of an acetyl group from a target protein or other molecule. This reaction is dependent on NAD^+ (Imai et al., 2000), and for this reason, sirtuins can act as a metabolic and redox sensor, as their activity is sensitive to the cell NAD^+/NADH ratio (Abdel Khalek et al., 2014).

Some studies have tried to bridge sirtuins and pluripotency/differentiation in ESC, via their histone deacetylation activity, as well as deacetylation of other proteins (Rodriguez et al., 2013). SIRT1 has been implicated in histone deacetylation, as the sirtuin with the highest histone-deacetylation capability. SIRT1 KO mice die either in late stages of development or shortly after birth (Cheng et al., 2003). By deacetylating their respective histones, SIRT1 deactivates and thus suppresses neuronal development-related genes (Calvanese et al., 2010). Concomitantly, inhibition of SIRT1 seems to promote differentiation of mouse iPSC in neuronal stem cells (Hu et al., 2014). Also, SIRT1 appears to also be relevant in a pluripotency context by deacetylating elements of the FOXO-family (Brunet, 2004), and p53 (Langley, 2002), mitigating their activity, which may facilitate differentiation (Gonzales and Ng, 2011; Li et al., 2012).

Some studies hint that the cytoplasmic sirtuin SIRT2 may influence neuronal differentiation through targeting the α-tubulin subunit of microtubules (Southwood et al., 2007). Other sirtuins have yet to be definitively linked to differentiation and/or pluripotency of ESC.

Sir-two homologue protein 3 – Sirtuin 3 (SIRT3) is a NAD-dependent lysine deacetylase. Of the seven known Sirtuins, SIRT3 has been shown to be predominantly at the mitochondria, where it regulates mitochondrial acetylation profiles. There are two other sirtuins in this organelle, SIRT4 and SIRT5, but it is believed that SIRT3 is responsible for 90% of total

mitochondrial deacetylation (Brown et al., 2013). SIRT3 activates the global mitochondrial metabolism by deacetylating key proteins in different metabolic pathways, namely in the Krebs cycle (Acetyl-CoA sintetase, Isocitrate Dehydrogenase 2, and Succinate Dehydrogenase, Succinate Dehydrogenase and Complex I), and also Antioxidant defense (Mn-SOD2). Therefore, SIRT3's primary action is the activation of mitochondrial metabolism. Along with these well-established roles, SIRT3 has been shown to regulate metabolic shift in cancer, as well as inducing proliferation of cancer stem cells. One study determined that SIRT3 appears to be necessary for *in vitro* differentiation of brown adipocytes, from HIB1B pre-adipocytes (Shi et al., 2005). Incidentally, SIRT3 is mostly expressed in brown adipose tissue, in adulthood. Thus, it would be of interest to assay if SIRT3 could have similar effects on mESC.

It is relevant to report that there are SIRT3 knockout systems available, with both SIRT3 KO cells and mice being commercialized. Studies performed on these systems show that both present overall similar phenotypes to their wild-type counterparts, the only difference residing in metabolic pathologies due to mitochondrial dysfunction (changes in ACeCS2, ATP levels and mitochondrial protein acetylation, deficient oxidative stress defenses) in older, KO mice model.

1.4 Silencing Mechanistic

There are different methods for silencing or suppressing a protein or its activity. Pharmacological inhibition is perhaps the first obvious tool to achieve this purpose. However, there are other more specific and effective methods for this purpose, notably involving genetic silencing, which considers both genetic knockout (gene KO, genetic information is deleted from the organism's genome, resulting in complete suppression of a protein) and knockdown (protein expression levels are diminished, usually by interfering with either DNA transcription, or mRNA stability/translation). Genetic knockdown (KD) is regularly achieved through the use of RNA interference (RNAi). RNAi consists in the use of small RNA nucleotides with sequences specific for an mRNA coding the protein of interest. There are several classes of interfering RNA molecules, namely shRNA (short-hairpin RNA), dsRNA (double-stranded RNA, avoided as it may activate interferon I pathway (Lambeth and Smith, 2013)), or siRNA (small interfering RNA). There is another RNAi system in the cell, which is natively used as part of its protein expression regulation, miRNA (microRNA). All of these interfering RNAs have similar mechanisms, in spite of slight differences between them, as their source or processing enzymes (Fellmann and Lowe, 2014).

After being transcribed from the transfected DNA sequence, shRNA is processed by Dicer (an endoribonuclease (RNAse III family), typically expressed by cells for their own native RNA-interference processes), giving rise to a siRNA (double stranded, with an anti-sense strand and a sense strand). siRNA binds to RISC (Ameres et al., 2007) (RNA-interference silencing complex), being the antisense strand used to recognize the target mRNA (the sense strand), and bind to it, as shown in Figure 8. Perfect binding to sequences result in cleavage and degradation of target mRNAs, whereas imperfect binding, commonly seen with miRNAs,

results in translational repression (Fellmann and Lowe, 2014). Both these effects are managed through the catalytic component of RISC, the Argonaute protein group (Ameres et al., 2007).

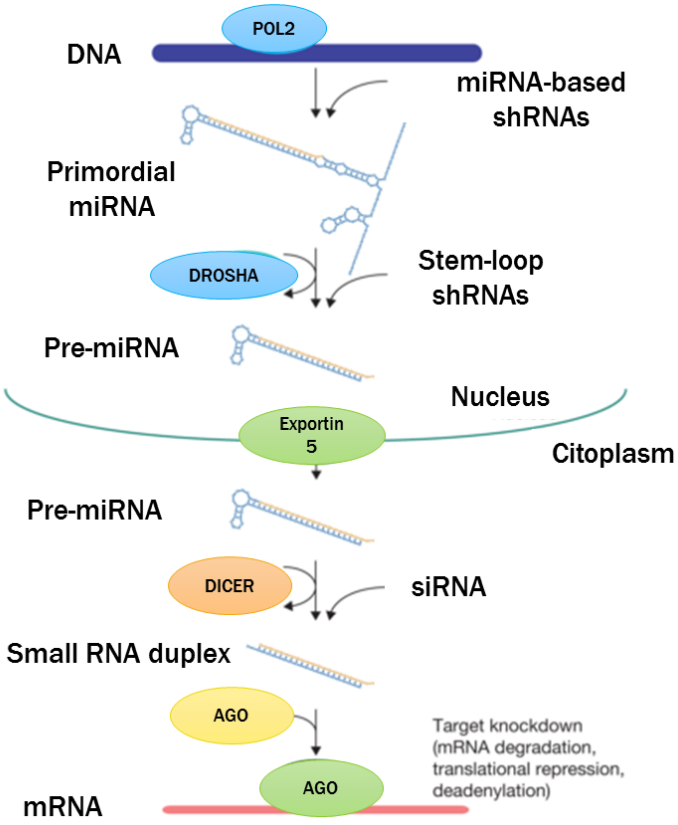

Figure 8 - Mechanism of shRNA silencing action. Pol II: RNA polymerase II. Ago: Argonaute protein. RISC: RNA-interference Silencing Complex. Adapted from: (Fellmann and Lowe, 2014)

Some of the advantages of shRNA KD over other silencing techniques include its relatively stable expression (compared to direct siRNA transfection, but still not as stable as when virus are employed), the fact that DNA delivery methodologies are well established, it is cost-effective advantageous for long-term experiments (cheaper than KO models), and provides an elegant solution for silencing proteins that may be crucial for the cell's regulation, in which a KO would result in immediate cellular death (Wittmann, 2006). The greatest advantage for this type of silencing is its adaptability for the target: having established a silencing protocol in a certain cell line, we can virtually silence any protein as long as a specific shRNA-containing plasmid is available. Therefore we aimed to introduce and optimize this method in our laboratory in order to be available as a tool to understand pluripotency and differentiation mechanisms of ESCs.

2 OBJECTIVES

The primary objective of this work was to establish a silencing protocol, via genetic knockdown in mouse Embryonic Stem Cells. This method was established by targeting a mitochondrial protein, Sirtuin3, with capacity for metabolism modulation, by transfection of a shRNA-expressing plasmid, ending with an evaluation of the knockdown level of the said protein.

3 METHODS

3.1 TASKS

3.1.1 Task #1 – Cell culture

The first task involved learning how to culture and maintain a mES cell line, E14Tg2.a, in which part of the study was performed. The prominence of this task is justified by its own complexity: mESCs culture requires a great amount of experience and awareness during their maintenance, as they are particularly sensitive to different stress stimuli, such as temperature, pH, nutrient availability, as well as various other different (toxic) molecules that can accumulate in the culture medium due to both normal cell metabolism and cell death, which can lead to its unwanted spontaneous differentiation.

An example of mESCs co-cultured with mouse embryonic fibroblasts (MEFs) can be seen in Figure 9. It should be noted that some cells are starting to leave its most pluripotent state (red arrows) relatively to blue-arrowed colonies (stronger pluripotent phenotype from the morphological point of view). In this figure it can be seen how heterogeneous a mES cell culture can be. It is possible that, in a good stem cell culture, up to 10% differentiation levels can be seen as acceptable. Pluripotent colonies are characterized by their round morphology, high optical refringence (brilliant, white borders), and small cell size. As these colonies start the differentiation process and lose their pluripotent phenotype, cells tend to spread away from the center of the colony, increasing their size, and decreasing refringence. Strict monitoring of the culture's pluripotent state is essential in the process of its maintenance, as well as confluence (higher or very low confluences may lead to spontaneous differentiation).

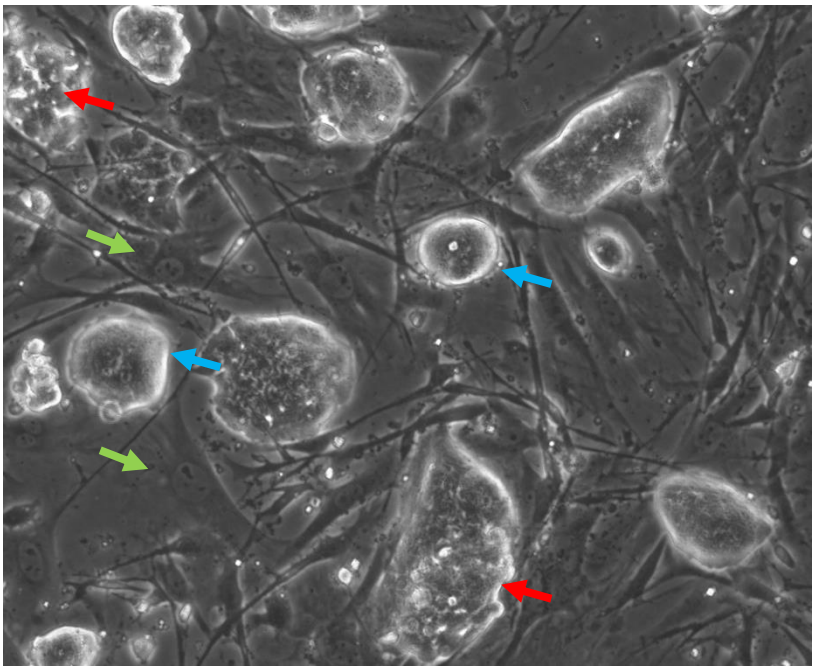

Figure 9 - Phase contrast microscopy of a mES R1 cell line co-cultured with MEFs. Examples of mESC colonies marked with blue arrows, a colony losing its pluripotent phenotype with reds arrows and MEF with green arrows.

Unlike mES R1 cells, E14Tg2.a cells do not require MEFs in order to proliferate and maintain pluripotency (Ward et al., 2004), and thus were be cultured in (0.1%) gelatin coated dishes, yielding cultures very much like those of Figure 3. Cells were be kept undifferentiated by adding Leukemia inhibitory factor (LIF) (1000 U / ml), as LIF integrates signals into mESC to maintain pluripotency (Niwa et al., 2009).

3.1.2 Task #2 – Plasmid choice, preparation and Lipofectamine® transfection

SIRT3 activates the global mitochondrial metabolism by deacetylating key proteins in different metabolic pathways in the mitochondria, and previous studies determined that SIRT3 appears to be necessary for *in vitro* differentiation of brown adipocytes (Giralt et al., 2011; Shi et al., 2005), it would be valuable to assay if SIRT3 could have similar effects on mESC.

In spite of the availability of a SIRT3 inhibiting drug, 4-hydroxynonenal (4-HNE), its inhibiting effect is not specific towards SIRT3, inhibiting other deacetylases and having targets beyond Sirtuins. Therefore, this pharmacological approach is unadvisable if SIRT3-specific silencing is desired. Additionally, the possible inhibitory effect of 4-HNE on SIRT3 was already tested in our laboratory, and no effect was seen, at least regarding mESC E14. Thereby, in this project we attempted to use a different and hopefully better solution to study the effects of SIRT3 on mESCs.

A group of four shRNA expressing plasmids (against different regions of SIRT3's mRNA, Genecopeia™ #MSH032833-LVRH1MP) was chosen for our silencing protocol. Cells will be grown in a puromycin containing medium. As each plasmid contains a puromycin resistance gene (antibiotic selection marker), only transfected cells will be able to survive and form

colonies. These plasmids also contain a fluorescent reporter gene, which allows us to directly monitor the plasmid's presence in the cells. Taken together, these elements aim to provide an effective RNA interference and knockdown of SIRT3's levels. This plasmid contemplates the possibility of genomic integration of the shRNA coding region via HIV infection, providing an alternative way of transfecting the cells. The use of shRNA is favored over siRNA and dsRNA as it mimics the endogenous miRNA pathway, therefore it is significantly more efficient, assures increased knockdown stability, and mitigates a possible activation of interferon I pathways. Moreover, DNA handling and delivery methods are easier and well established in literature for mESC. Nonetheless, shRNA technologies are not devoid of disadvantages, as they require either a frequent re-acquisition of the plasmids, or expansion of plasmids in bacteria, and thus, conditions to work and manipulate bacteria.

Plasmids were expanded in *E.coli* and transfected in mESC using lipofectamine-mediated transfection. This method takes advantage of the interaction between the positive charges of lipofectamine and the negative charges of the plasmidic DNA. The resulting complex is then internalized into the cell. The choice of this transfection protocol above others of the kind (electroporation, heat shock) is due to the reported efficiency for the stem cell line E14Tg2.a (Christophorou et al., 2014).

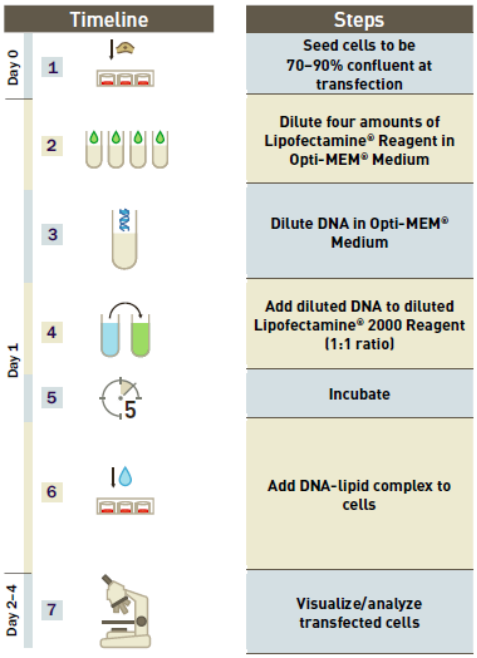

Figure 10 - Transfection protocol for Lipofectamine® mediated transfection. (Lipofectamine® 2000 DNA Transfection Reagent Protocol)

E14Tg2.a cells were transfected in the third day after passaging, using the Lipofectamine 2000® (Invitrogen™) reagent as described in the manufacturer's protocol (Invitrogen(tm) by

life technologies, 2000), shown in Figure 10, and later with Lipofectamine® 3000, using a similar protocol.

3.1.3 Task #3 – Assay for knockdown effectiveness and stability

In order to assay knockdown effectiveness and stability, both Western Blot and qRT-PCR were employed.

Quantitative Reverse-Transcription Polymerase Chain Reaction (qRT-PCR), which allows us to measure the expression and the existing amount of a given mRNA strand, by using the appropriate primers, was applied to conclude about the levels of SIRT3's coding mRNA in the cell. Nonetheless, taking into account that shRNA silencing can culminate with both the degradation of the target mRNA or solely the repression of its translation by rRNA (the multitude of effects is dependent of the Argonaute protein present in the catalytic domain of the RISC complex), SIRT3 mRNA levels may or may not be significantly different between KD and control cases.

After collecting the total protein contents of transfected cell cultures, SIRT3 levels were be measured by Western Blot.

In order to perform the two aforementioned techniques, both the protein and mRNA contents of cultured cells were collected. In case of a successful SIRT3 knockdown, the same protein and mRNA samples would be used to measure the expression of pluripotency markers such as Nanog and Oct4, thus allowing to infer on how SIRT3 may or may not affect pluripotency, and also differentiation.

Being a lysine deacetylase responsible for the acetylation of 90% of mitochondrial proteins (Lombard et al., 2007), and taking into account that SIRT3 primarily operates in this organelle, SIRT3 KD cells should reveal increased acetylation in their mitochondrial proteins. This measurement was possible by using an antibody against Acetylated lysine (a measure of activity), by Western Blot analysis.

3.2 CELL LINES, CELL CULTURE AND DIFFERENTIATION

E14Tg2.a mES cell line was chosen to perform all ESC assays. mESCs were cultured in 0.1% gelatin-coated dishes, with the denominated "KODMEM medium" consisting in Knockout™ Dulbecco modified Eagle medium (Gibco #10829-018) supplemented with 15% Knockout Serum Replacement (KSR; Gibco #10828-028), 1000 U/mL LIF (Merckmillipore #ESG1107), 100U/mL penicillin, 100 µg/mL streptomycin (Gibco #151910-122), 2 mM L-Glutamine (Gibco #25030-024), 0.1 mM non-essential amino acids (Sigma #M7145), and 0.1 mM β-mercaptoethanol (Sigma M17522-100mL) at 37°C / 5% CO_2. Media was replaced daily, and cells passaged every 2 to 3 days, with a density of 6000 cells/ cm^2. StemPro® Accutase® (Gibco #A1110501) was used as dissociation agent. Briefly, old culture medium was removed, and the cells were then rinsed with warm PBS, and accutase was added. After a 5 minutes incubation at 37°C, new, warm culture medium was added to inactivate the enzyme, and cells were collected into a 15mL conical tube. Then, cells were centrifuged at 200g for 5 minutes at room temperature. Supernatant was discarded, and the cells were then resuspended in KODMEM. Cells were then counted as described in section 3.4.3, and the appropriate volume containing the wanted cell number was plated in a new, gelatin coated dish with warm KODMEM.

Non-directed differentiation into embryoid bodies (EBs) was made using E14Tg2.a cells. This differentiation was conducted to assay changes in the expression of both pluripotency and differentiation markers. Therefore, 10^6 cells were plated in non-adherent 60mm dishes with 5 mL KODMEM medium. Cells were then incubated for 3 days at 37°C and 5%CO_2, while replacing the culture medium daily. At the third day, EBs were plated in 100mm tissue-culture dishes coated with 0.1% gelatin, with 10% Fetal Bovine Serum (FBS, Gibco #10270-106))-supplemented KODMEM culture medium. On the following day, "normal" KODMEM culture medium was added and medium was daily replaced from the fourth day onwards. Total protein contents were collected every two days during 14 days of protocol.

A differentiated cell line (NIH-3T3, mouse embryonic fibroblasts), 3T3, was employed to validate that the plasmid and as a control for the low efficiency of transfection. 3T3 cells were grown in Dulbecco modified Eagle medium, hereby referred to as "DMEM medium", consisting of DMEM (DMEM, Gibco #41965-039) with 10% FBS, 100U/mL penicillin, 100 µg/mL streptomycin, 0.1 mM nonessential amino acids, and 1mM sodium pyruvate (Gibco #11360-039), while being incubated at 37°C and 5% CO_2. Cells were detached with TrypLE (Gibco #12605-028), and passaged with dilutions ranging from 1:30 to 1:60, when 70-80% confluence was achieved. The passaging protocol is very much alike the one described for mESC: DMEM medium was removed, cells were washed with warm PBS and TrypLE was added. After a 5 minutes incubation at 37°C, new, warm culture medium was added. Cells in suspension were collected into a 15mL conical tube. Then, cells were also centrifuged at 200g for 5 minutes. The supernatant was removed, and the cells were then resuspended in new DMEM. Cells were then counted; the appropriate volume of cells was plated in new, cell culture flasks with DMEM.

3.3 *E.COLI* TRANSFORMATION; PLASMID AMPLIFICATION, ISOLATION AND ANALYSIS

LB-agar plates for bacterial culture were prepared following the manufacturer's instructions (Nzytech #MB14502) in 90mm bacterial dishes. Briefly, 50g of LB broth (Nzytech #MB14502) and 40g of agar (Becton Dickson #214050) per liter of distilled water were sterilized through autoclaving (121°C for 45 minutes). Following this process, the broth was kept at 60°C, averting solidification. The appropriate antibiotic was then added to get a final/working concentration of 100 μg /mL for carbenicillin (Fisher Scientific #BP26481) or 50 μg /mL for kanamycin (AcrosOrganics® #450810100), whenever the LB-agar plates were meant for antibiotic-based selection. Approximately 20mL of LB-agar broth was poured directly into the 90mm bacterial dishes, in sterile conditions (flux chamber), and left to cool until solidification. Each dish was then inverted (lid facing down), date, user, antibiotic name and concentration were written, and lastly, sealed with parafilm (PARAFILM #05170002). Sealed sterile dishes were kept in a sealed bag at 4°C until needed.

E. coli was transformed via the heat-shock transformation protocol (Nzytech, 2013). 40 μL of glycerolated stock NZY*5α E.coli* (Nzytech #MB00401) was transfected with 2ng of plasmidic DNA. The eppendorf containing the bacteria and DNA was incubated on ice for 5 minutes and then, heat-shocked in a water bath at 42°C for 45 seconds. After, the eppendorfs were returned to ice for another 2 minutes. 500 μL SOC broth (Nzytech #MB11901) was then added to each eppendorf and incubated in a 37°C incubator with agitation for 20 minutes, allowing bacteria to recover from the ice-heat cycles. 150 μL were plated in LB-agar plates with 100 μg /mL carbenicillin or 50 μg /mL for kanamycin, which allows plasmid positive and negative (respectively) *E.coli* selection, as the chosen plasmids encode for an ampicillin/carbenicillin resistance-conferring gene. A Bunsen burner was employed to achieve sterile conditions and thus minimize contamination chances of all reagents and materials.

Plasmid amplification was attained by two steps of *E.coli* culture. Plasmid-positive colonies were picked early in the morning to a 15 ml falcon tube containing 5 mL SOC broth with 100 μg /mL carbenicillin, and incubated at 37°C and 180 rpm, over day. Then, the pre-culture was transferred to a 500 mL Erlenmeyer flask with 200mL SOC broth with 100 μg /mL carbenicillin and incubated overnight in the aforementioned conditions. Next morning, *E.coli* were harvested (by centrifuging the bacterial suspension, at 4000g) in order to perform DNA isolation via the PureLink® HiPure Plasmid Filter Maxiprep Kit (Invitrogen #K2100-17). This isolation process includes the sequential additions of kit buffers, such as RNAse containing buffers. The procedure was performed as recommended by the manufacturers.

After elution of the DNA-binding columns, the isolated DNA was precipitated with 2-propanol (Sigma #59304-1L-F) and centrifuged at 16000g for 30 minutes. The supernatant was discarded; the pellets were rinsed with 70% ethanol (MerckMillipore #1085430250) and then centrifuged again at 16000g for 10 minutes. Ethanol was removed; the DNA pellets were left to dry, and then resuspended in Molecular Biology-grade water (MerckMillipore #H20MB0501).

DNA concentration was determined via a *NanoDrop®* 1000 Spectrophotometer. Molecular Biology-grade water was used as blank for the measurements, and 1 μL of DNA solution was pipetted in order to determine the concentration and purity of the nucleic acid. Following this procedure, DNA samples were aliquoted and kept at -20°C pending use.

3.4 SELECTION CONDITIONS

3.4.1 Antibiotic Concentration

The minimum concentration of puromycin that was able to kill every cell/colony was determined in order to select plasmid-positive cells/colonies. As the chosen plasmid for transfection carries a puromycin resistance-conferring gene (PAC - puromycin *N*-acetyl-transferase), an enzyme that disables the inhibition of protein synthesis from puromycin, by acetylation of a moiety of the said antibiotic (Gómez Lahoz et al., 1991; Vara et al., 1985)), successfully transfected cells must be resistant to concentrations of puromycin that would otherwise kill them. So, both non-transfected cell lines were plated in 12-well plates and cultured in the presence of increasing concentrations of puromycin (ranging from 0.5 μg/mL to 2.5 μg/mL. Puromycin concentrations were chosen according to existing data (Aubert et al., 2002; Chambers et al., 2003; Conti et al., 2005; Simsek et al., 2010; Wang et al., 2007; Zhang et al., 2006)). Then, cells were treated with different concentrations of puromycin, 24 hours after plating. Antibiotic selection was conducted for 3 days (ESCs) and 7 days (3T3). The next step was to determine the antibiotic's effectiveness by cell counting under a microscope, and Sulforhodamine B colorimetric assay.

3.4.2 Sulforhodamine B (SRB) colorimetric assay

Cells were fixed with 4% Para-formaldehyde (Sigma #P6148-500G) for 15 minutes at room temperature. After removing the fixative solution, cells were washed with PBS for three times, 5 minutes each. PBS was then removed and the plate was allowed to dry overnight. In the following day, 500 μL of 0.1% SRB (Sigma #S9012-256) solution was added to each well containing cells exposed to different concentrations of SRB. After an incubation period of 1 hour at 37°C, the SRB solution was removed, and washed trice with a 1% acetate solution. Following this step, the plates were left to dry overnight, at room temperature. Next day, 1 mL of 10mM TRIS, pH=10 buffer was added to each well. The plates were then subject to stirring for 15 minutes. From each well, 200 μL of the TRIS buffer was collected to a transparent, 96-well plate, and read with a spectrophotometer (at 540nm) in order to determine the amount of remaining SRB, which had bound to proteins, and would give a measure of total protein content.

3.4.3 Cell counting

Cell counting allowed the quantification of the number of surviving cells in each selecting condition. Cells were detached with either Accutase® (E14 cells) or TrypLE™ (3T3 cells), having previously rinsed the cells with PBS, to ensure maximum enzyme activity. Following the addition of the detaching agent, both cell lines were incubated at 37°C for 5 minutes. The detaching action of both reagents was inhibited with the addition of culture medium (with a total volume of 4 times the volume of detaching enzyme employed), and the cell suspension was collected then centrifuged at 1200 rpm for 5 minutes. Supernatant was promptly discarded and the cells were ressuspended in 1 mL of the corresponding culture medium. An aliquot of 20 µL was mixed with 20 µL of Trypan Blue Solution, 0.4% (Sigma #T8154). A total volume of 10 µL of the resulting cell suspension was pipetted to a Nebauer Improved Counting Chamber (Marienfeld #0610010, as shown in Figure , with 0.1 mm of depth) and counted under a microscope. The four outer quadrants (with 1mm^2 areas) were counted.

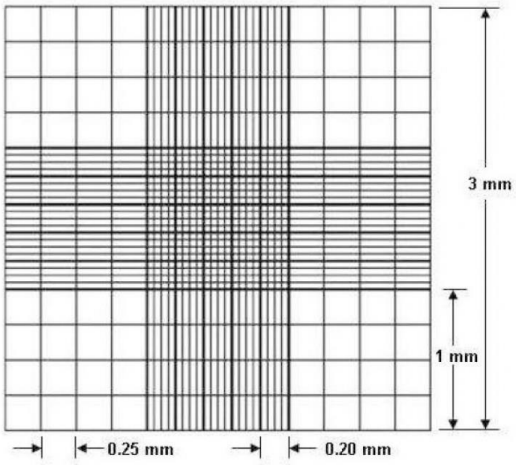

Figure - Grid size for the Nebauer Improved Counting Chamber.

The total number of counted cells is calculated according to Equation 1. As each quadrant has an area of 1mm^2, and a depth of 0.1mm, the corresponding volume, per quadrant, is of 0.1mm^3 (1mm*1mm*0.1mm), or 0.1µL. In order to obtain a cell concentration in the order of the mL, the total number of cells must thus be multiplied by 10000. Four quadrants were counted in order to decrease the chance of systematic counting errors, which implies that the total number of cells counted (in the four quadrants) must be normalized to obtain a fixed number of cells per quadrant. As cells were diluted in Trypan Blue prior to counting, this dilution must be taken into account.

$$Cell\ concentration\ \left(\frac{cell}{mL}\right) = \frac{\#cells\ counted}{\#quadrants\ counted} * 10000 * dilution \qquad [1]$$

After obtaining the total number per condition, those values were divided by the number of cells in the control condition and the result is expressed in a percentage of live cells relatively to control, as calculated using Equation 2.

$$Percentage\ of\ surviving\ Cells = \frac{\#cells\ in\ culture}{\#cells\ in\ control} * 100 \quad [2]$$

3.5 TRANSFECTION

Both cell lines were transfected using Lipofectamine 2000 (Invitrogen #11668-030) and Lipofectamine 3000 (Invitrogen L3000-008) reagents. Transfection was made according to manufacturer's instructions, albeit modified.

Cells were passaged as described, and seeded on 12 well plates at 15000 cells per cm^2 (NIH-3T3 cells) and 5000 cells/cm^2 (E14Tg2.a cells), with 1 mL of the corresponding culture medium (KODMEM for E14 cells and DMEM for 3T3 cells). Concomitantly, different ratios of DNA:Lipofectamine (DNA mass: Lipofectamine volume) were tested, starting with 0.5 μg of Plasmidic DNA.

Two references of Lipofectamine were used: Lipofectamine 2000 and Lipofectamine 3000. DNA and Lipofectamine 2000 solutions were prepared, separately, by dilution in OptiMEM medium (Gibco #31985-047). Each mixture was incubated at room temperature for 5 minutes, before adding the contents of the DNA-OptiMEM tube to the Lipofectamine 2000-OptiMEM containing tube. This DNA-Lipofectamine 2000-OptiMEM mixture was then incubated for another 5 minutes at room temperature in the dark, and finally added to each well dropwise. The plates were incubated at 37°C, 5% CO_2 overnight. On the next day the plates were assayed for the emission of fluorescence (caused by expression of mCherry), and 1 mL of culture medium was added. On the third day, the culture was monitored for fluorescence and confluence the culture medium was removed and replaced with fresh culture medium supplemented with puromycin in order to select plasmid-positive cells.

Transfection with Lipofectamine 3000 followed the same guidelines, except the addition of the reagent dubbed "P3000 reagent" to the DNA-OptiMEM mixture. For each μg of DNA added, 2 μL of P3000 reagent were added. With both methods, following antibiotic selection, cells were passaged, as described, for wild type E14 and 3T3 cells.

3.6 FLOW-CYTOMETRY

Flow-cytometry was performed with transfected 3T3 cells in order to quantitatively evaluate transfection efficiency. The transfection efficiency could be measured through the

red fluorescence of positively transfected cells, conferred by the mCherry-expressing plasmid. Therefore, 3T3 cells (two samples of transfected and non-transfected cells) were detached with TrypLE, as described. Following the centrifugation step, the supernatant was discarded and the cell pellet was resuspended in warm PBS, and analyzed with a BD FACSCalibur flow-cytometer. For each "cell line", a total of 20.000 events were recorded. After a quick run, the aberrant cells and cellular debris was gated out, based on light scattering, and by designing a region that only included those who were considered to possess a "normal" forward and side light scattering. Red fluorescence (mCherry absorbs at the wavelength of 387nm, emitting maximally at 610nm) was promptly measured in the FL2 channel. Data was analyzed using the Cell Quest Pro Acquisition software, and the percentage of Fluorescent/non-fluorescent 3T3 cells was calculated.

3.7 RNA

3.7.1 RNA isolation

Cells were washed with warm PBS and the adequate detaching agent was added. After a 5 minutes incubation period at 37°C, medium was added to inactivate the enzyme, and cells were collected into a 15mL conical tube. Then, cells were centrifuged at 200g for 5 minutes at room temperature. Supernatant was discarded; cells were washed in PBS 1x and centrifuged again.

Afterwards, in an RNAse free environment and using RNAse-free pipette tips, pipettes, and eppendorf tubes, the supernatant was removed, 1 ml of TRIZOL reagent (Invitrogen #15596026) was added and the samples were vortexed for 10 seconds. Then, 200 µL of chloroform (Sigma #C242-25mL) was added to the mixture, and vortexed for 30 seconds. The samples were then centrifuged at 4000 rpm for 5 minutes (room-temperature), and the transparent/aqueous phase was collected to an RNAse/DNase-free eppendorf tube, without disturbing the phenol red-containing phase. Lastly, 600 µL of isopropanol were added to each eppendorf tube, the tubes were labeled and kept at -20°C, until DNA clean-up.

3.7.2 DNA cleanup, quantification and first strand cDNA synthesis

Following the isolation step, RNA samples were centrifuged at 16.000g at 4°C for 30 minutes, and the resulting supernatant was discarded. 1ml of 75% ethanol, previously prepared with molecular biology-grade water, was added and the RNA samples were centrifuged at 16000g at 4°C for 10 minutes. The supernatant was discarded and the pellets were left to air-dry. 20 µL of nuclease-free water was added. These samples were then ready to undergo DNA clean-up. DNAse I buffer (0.2 µL, Ambion #816962)) and rDNase I (2 µL, Ambion #2224G) were then added to the RNA samples, and the contents were gently mixed. These RNA-containing tubes were incubated at 37°C for 30 minutes. After, DNAse Inactivation reagent (0.2µL, Ambion #8174G) was added to each sample, and incubated at room temperature for 2 minutes, while mixing occasionally. Finally, the samples were centrifuged

at 10.000g for 1.5 minutes, and the RNA-containing supernatant was transferred to a new, labeled, RNAse free tube.

The resulting RNA was then quantified via *Nanodrop®*, as described before, albeit choosing a different quantification profile (one adequate for RNA instead of DNA).

In order to perform cDNA synthesis, a reaction mix with a total volume of 20 µL, containing 4µL of iScript reaction mix (BIORAD #170-8890), 1µL iScript reverse transcriptase (BIORAD #720001205), and the volume equivalent to 1.5µg of RNA (20µL total volume was achieved by adding Nuclease free water), was prepared in PCR-ready tubes. These tubes were then subject to the PCR reaction, with the definitions shown in Figure 11.

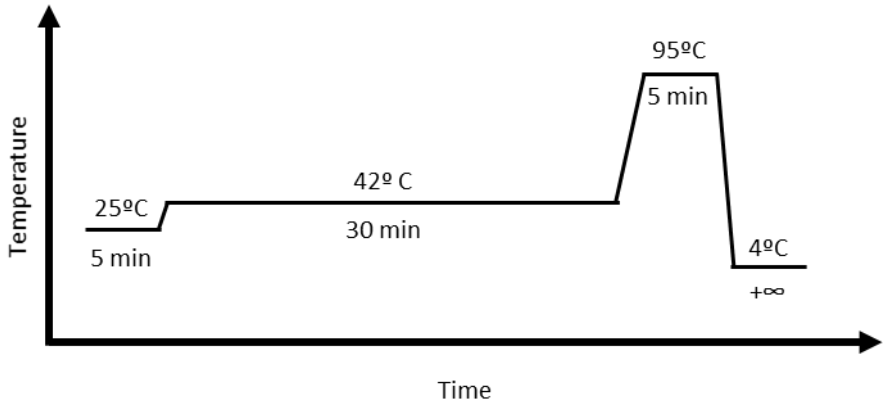

Figure 11 - Thermocycler definitions for cDNA synthesis.

3.7.3 qRT-PCR

The expression of four genes was evaluated through qRT-PCR, and the resulting expression was normalized to β-actin. The three-mitochondrial sirtuins (SIRT3, SIRT4 and SIRT5) had their mRNA equivalent measured, as well as SIRT1, the most widely studied sirtuin. The primers chosen and ordered for this step of the protocol are shown in Table 1. The sequences were obtained from the PrimerBank database (http://pga.mgh.harvard.edu/primerbank/), and the primers were ordered from Integrated DNA Technologies (IDT).

Table 1 - Identification and characterization of the primers chosen to perform qRT-PCR.

TARGET GENE	FW/RV	SEQUENCE	AMPLICON SIZE (BP)	PRIMERBANK ID
β-ACTIN	Forward	GGCTGTATTCCCCTCCATCG	154	6671509a1
	Reverse	CCAGTTGGTAACAATGCCATGT		
SIRT1	Forward	GCTGACGACTTCGACGACG	101	9790229a1
	Reverse	TCGGTCAACAGGAGGTTGTCT		
SIRT3	Forward	ATCCCGGACTTCAGATCCCC	126	11967963a1
	Reverse	CAACATGAAAAAGGGCTTGGG		
SIRT4	Forward	CAAGAAACTCCTCGTGATGACA	97	267844848c2
	Reverse	GTCAGTGCGGGCGTAAAGT		
SIRT5	Forward	CTCCGGGCCGATTCATTTCC	130	30578432a1
	Reverse	GCGTTCGCAAAACACTTCCG		

For each gene to be analyzed, a master mix (with a total volume of 20µL) was prepared by adding: 10µL SsoFast™ EvaGreen® Supermix (Biorad #750000117); 1µM of both Forward and Reverse primers, cDNA template of the desired sample, and 5µL of nuclease free water, to a 96 well RT-PCR plate (Biorad). qRT-PCR is run in CFX96 Touch™ Real-Time PCR Detection System, and mRNA fold change was calculated using the -ΔΔCt method.

3.8 Protein Expression Analysis

3.8.1 Immunocytochemistry

Cells were plated at 10.000 cells/cm2 in cell culture 13mm coverslips (Thermanox 174950) and grown for three days. The cells were then fixed with 4% paraformaldehyde in PBS for 15 minutes, at room temperature. After fixation, cells were washed with cold PBS and kept at 4°C in 0.1% sodium azide in PBS 1x, pending use. For the immunocytochemistry protocol *per se*, cells were firstly permeabilized and blocked with a 1% Triton-X100 and a 3% BSA, solution in PBS respectively, for 30 minutes. Cell-containing coverslips were incubated with the primary antibodies (antibodies employed can be consulted in Table 2) overnight diluted in a 1% BSA, 0.25% Triton-X in PBS solution. In the following morning, the coverslips were incubated with the corresponding secondary antibody for 1h at room temperature, after three washes in PBS for 5 minutes each. Incubation with Hoechst 33342 (to allow staining of the nucleus) was also performed, diluted 1:1000 in PBS, for 10 minutes at room temperature. Cell-containing coverslips were washed three times with PBS before mounting. Samples were mounted in slides with a drop of Vectashield® (Vector H1000) with a glass coverslip, and sealed with nail polish to prevent samples from drying.

Table 2 - List of Antibodies used in immunocytochemistry, their sources, and dilutions.

Antibody	Strain	Manufacturer	Reference	Dilution	Incubation Time
OCT4	rabbit	Cell Signaling	#2840	1:750	overnight
SOX2	goat	Santa Cruz	sc-17320	1:500	overnight
TOM-20	rabbit	Santa Cruz	sc-11415	1:200	overnight
SIRT3	rabbit	Abcam	ab86671	1:1000	overnight

3.8.2 Western Blot

3.8.2.1 Protein Extraction & Quantification

Total protein content was obtained from cell extracts for later characterization through Western Blot. Cells were washed with PBS, and detached with either Accutase® (for E14 ES cells) or TrypLE® (for 3T3 cells), centrifuged at 200g for 5 minutes. The pellet was washed with PBS and centrifuged again. Having discarded the supernatant, the pellet was then digested with RIPA® buffer (Sigma #R0278-50mL) supplemented with protease inhibitors (Protease Inhibitor Cocktail (Sigma #P8340) and PMSF (Sigma #78830)) and phosphatase inhibitors (Thermo Fisher Scientific #78830) for a minimum of 5 minutes, on ice. Following this process, samples were centrifuged at 500g for 15 minutes. The supernatant was carefully collected to a 1.5 ml eppendorf tube, labeled, and stored at -80°C. Protein concentration must be determined before sample preparation for blotting, to allow the loading of 30 µg of protein into each well, to standardize the amount of protein in each lane/sample. Protein concentration determination for each sample was accomplished using the Pierce™ BCA Protein Assay Kit.

3.8.2.2 Western Blot

Quantified protein extracts were subject to sodium dodecylsulphate polyacrylamide gel electrophoresis (SDS-PAGE), in a 12% acrylamide gel and the electrophoretic conditions were selected according to the characteristics of the proteins of interest. Protein samples were denatured prior to the electrophoresis. In order to do so, 30 µg of protein from each sample (determined after the quantification process) were diluted in water and to each tube, an equal volume of Laemmli buffer (BioRad #161-0737) with β-mercaptoethanol (Sigma M7522-100mL) (a denaturing buffer) was added. The protein samples were then subject to heating, at 70°C, for 10 minutes, and vortexed for 1 minute afterwards. Electrophoresis gels were prepared accordingly to Table 3 (running gel portion) and Table 4 (stacking gel portion).

Table 3 - Chemical components of the Acrylamide running gel for protein electrophoresis.

REAGENT/SOLUTION	VOLUME (PER GEL)
ddH_2O	3.4 mL
40% ACRYLAMIDE (BIORAD #161-0148)	2.4 mL
1.5M TRIS, pH 8.8 (BIORAD #161-0798)	2 mL
10% SDS (BIORAD #161-0418)	80 µL
10% APS (BIORAD #161-0737)	80 µL
TEMED (BIORAD #161-0800)	8 µL

Table 4 - Chemical components of the Acrylamide stacking gel for protein electrophoresis.

REAGENT/SOLUTION	VOLUME (PER GEL)
ddH_2O	2,48 mL
40% ACRYLAMIDE (BIORAD #161-0148)	0.4 mL
0.5M TRIS, pH 6.8 (BIORAD #161-0799)	1 mL
10% SDS (BIORAD #161-0418)	40 µL
10% APS (BIORAD #161-0737)	40 µL
TEMED (BIORAD #161-0800)	4 µL

After polymerization, the gel was placed in an electrophoresis buffer chamber. Denatured samples were loaded into each well (30 µL, with 30 µg protein), as well as 5 µL of the adequate protein standard/ladder (Precision Plus Protein™ Dual Color Standards #161-0374). Electrophoresis was carried out with TGS buffer (10x Tris/Glycine/SDS #161-0772). Firstly, electrophoresis is run at 60V for 30 minutes, allowing the steady and efficient incorporation of the protein samples in the stacking gel, and at 140 V, for approximately one hour allowing the separation by size of the loaded proteins. In the meantime, PVDF membranes were activated with methanol (AppliChem Pancreac #131091.1212) for 15 seconds, then with water for 5 minutes, and lastly with transfer buffer (whose constituents are shown in Table 5) for at least 15 minutes, always under stirring.

Table 5 - Electrotransference buffer chemical constitution.

REAGENT	CONCENTRATION / VOLUME
TRIS-BASE (SIGMA #T150-1KG)	25mM
GLYCINE (SIGMA #G7126-1KG)	190mM
METHANOL (APPLICHEM PANCREAC #131091.1212)	200 mL
DISTILED WATER	Enough to 1 L of transfer buffer

Following electrophoresis, proteins were electrotransfered from the acrylamide gel to a PVDF membrane. All the components of the "electrotransference cassette" of the Mini Trans-Blot cell (BIORAD) were also soaked in transfer buffer, and then mounted as shown in Figure 12. After the assembly of the cassette containing both the electrophoresis gel and the PVDF

membrane the electrotransference (BIORAD Tetra Blotting Module), was conducted at 4°C, at 140V for 90 minutes in a BioRad Tetra Blotting Module. In order to improve the efficiency of the process and the integrity of the electrophoresis gel, the electrotransference system was immersed in ice. Also, to assure the homogeneity of the electrotransference buffer, the electrotransference system was coupled with magnetic stirring.

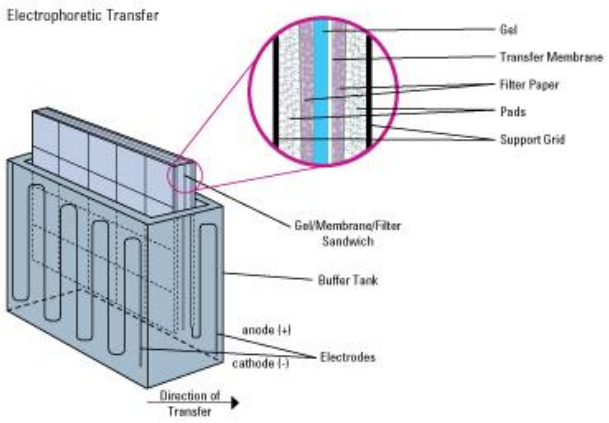

Figure 12 - Electrotranfer system scheme (https://www.lifetechnologies.com/content/dam/LifeTech/Images/integration/PDetectFig24_400x.jpg)

In the end of the electrotransference process, the PVDF membrane containing the transferred proteins was briefly washed in TBS-T solution (whose constitution is presented in Table 6).

Table 6 - TBS-T constituents

REAGENT	**CONCENTRATION / VOLUME (PER LITRE OF SOLUTION)**
TRIS-BASE (SIGMA #T150-1KG)	2,42 g/L
NACL (SIGMA #S7653-1KG)	8g/L
TWEEN-20 (BIORAD #161-0781)	10mL

Before incubation with the desired antibodies, the membrane must be blocked with 5% non-fat milk/blocking regain in TBS-T, for one hour at room temperature. Primary antibody incubations were carried out overnight, at 4°C. Antibodies were diluted in 5% non-fat milk in TBS-T to the desired concentration. The list of antibodies employed, as well as their dilution and manufacturer, can be seen in Table 7. The following morning, the antibody was collected and the membrane washed in TBS-T, three times exchanging the TBS-T solution every 10 minutes. The corresponding secondary antibody was diluted in 5% non-fat milk (BioRad #170-6404) in TBS-T, as done with the primary antibody, and incubated for 1 hour at room temperature. In the end of this incubation period membranes were washed with TBS-T as described.

Table 7 - List of Antibodies used in immunocytochemistry, their sources, and dilutions

Antibody	Strain	Manufacturer	Reference	Dilution	Incubation Time
AFP	rabbit	Cell Signaling	#2137	1:400	overnight
αSMA	mouse	Abcam	Ab7817	1:600	overnight
OCT4	rabbit	Cell Signaling	#2840	1:750	overnight
β-ACTIN	mouse	Sigma-Aldrich	A2228	1:25000	1 hour
SOX2	goat	Santa Cruz	sc-17320	1:500	overnight
SIRT3	rabbit	Abcam	ab86671	1:1000	overnight
SIRT1	mouse	Sigma-Aldrich	s5196	1:1500	overnight
ACLYS	rabbit	Cell Signaling	#9441	1:1000	overnight
TOM-20	rabbit	Santa Cruz	sc-11415	1:200	1 hour

The revelation step was carried out with ECL (GE Lifesciences RPN2235), in a BioRad® Versadoc™ apparatus. The membrane was incubated with ECL for a standard time of 5 minutes, protected from the light. Regarding the exposition settings in the Versadoc™ apparatus, they ranged from 10 to 30 seconds. When either over or underexposure was detected, these exposition periods were adapted. In the case of β-actin labelling, the very incubation time with ECL was reduced to decrease the chance of overexposure. Quantification of Western Blot images was carried out with the Quantity One® (by Bio-Rad) software.

4 RESULTS AND DISCUSSION

4.1 MESC CULTURING

4.1.1 Pluripotency in mouse Embryonic Stem Cells

mESC cultures are, to say the least, more sophisticated than other cultured cells. These cultures require daily medium exchange, while always monitoring the morphology, size and density of stem cell colonies. This is due to the fact that mESC cultured in the absence of feeder cells tend to differentiate in a spontaneous manner. They are also very sensitive to sudden changes in their environment: temperature, acidity, micronutrient concentration, and so on. While many other cell cultures only require passaging when certain levels of confluence are reached, mESCs morphology must be followed, as it is, by itself, a good indicator of the level of "stemness" of the colonies. When passaging, these cells must be plated within certain density values: if plated too densely, mESC will tend to differentiate (more on mESC differentiation ahead); and if plated too sparsely, the cells won't be able to form colonies and will eventually differentiate or die.

As a result, the culture medium for mESC culturing must be well defined and favor not only growth, but also pluripotency. KSR replaces the more common form of serum, FBS, in order to avoid unwanted animal contaminants (such as cytokines) present in the serum itself, as they may lead the cells to differentiate (Cheng et al., 2004). β-mercaptoethanol, which acts as an antioxidant, helps to regulate the redox potential of the culture medium and also contributes towards stem cell pluripotency, allegedly through sequestration of reactive oxygen species, and creating conditions that allow the uptake of cysteine (this uptake is easier in reductive environment, and cysteine and its metabolism are important for endogenous redox balancing (Bannai, 1992; Janjic and Wollheim, 1992)). The medium's base is KODMEM, as opposed to the usual DMEM, as it contains less serum-derived animal contaminants. In conclusion, all these components increase the quality of the stem cell culture, causing them to be notoriously expensive when compared to traditional cell lines.

Figure 13 shows microphotographs of E14 mESC cultured in two different conditions, with LIF (images A, B, and C) and without LIF (D, E and F), up to three days after passaging, and the most distinguishable characteristic of both groups is colony morphology: colonies cultured in pluripotency-sustaining conditions (i.e. with LIF) are rounder, have smaller cells (visually indistinguishable at this magnification), and light refraction is very different, when comparing to the less pluripotent colonies, which resembles which is commonly referred in the literature (Cahan and Daley, 2013). While maintaining E14 mESC cells in culture, one must seek to passage when colonies are rather large (in order to assure enough cells to maintain the culture and also plate for the ongoing experiments), but still pluripotent. As stated before, such can only be attained if the culture is strictly monitored.

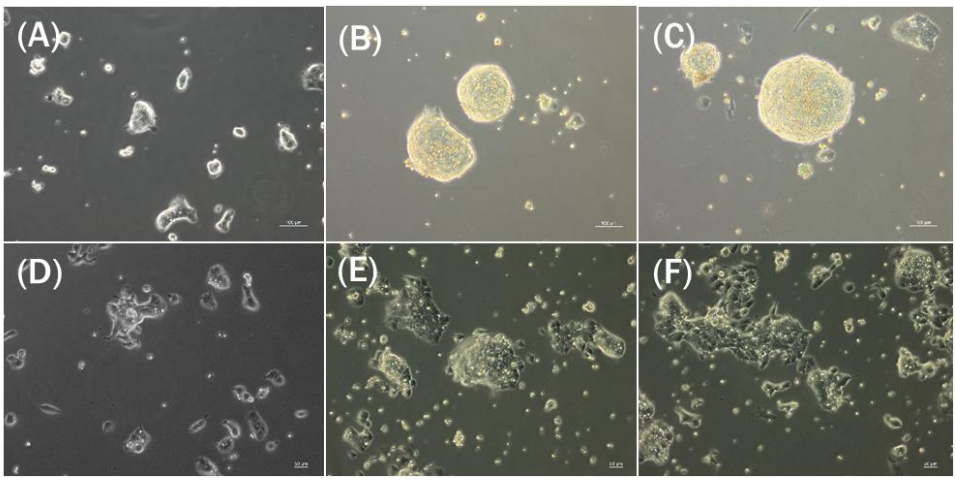

Figure 13 – Microphotographs of mESC cultures in different days after passaging, and with and without added LIF. Figures A, B and C refer to mESC cultured in KODMEM supplemented with LIF, 1, 2 and 3days after plating, respectively. Figures D, E and F present the same cell line cultured in KODMEM but with no LIF supplementation. Scale bar is 100µm.

Nevertheless, there are other, more accurate means to determine the pluripotency (or "stemness") of a cell culture. ESCs possess various specific markers that indicate their pluripotency, such as transcription factors OCT4, SOX2 and NANOG ("pluripotency core"). Therefore, immunocytochemistry was performed on both LIF-supplemented and non-supplemented E14 cultures, to show that the morphology observed in the previous figure is concomitant with the stronger or weaker pluripotent phenotype. In Figure 14 shows the results for this technique. The first row of each sets of images refer to ESC cultured with LIF, the second, cultured without LIF.

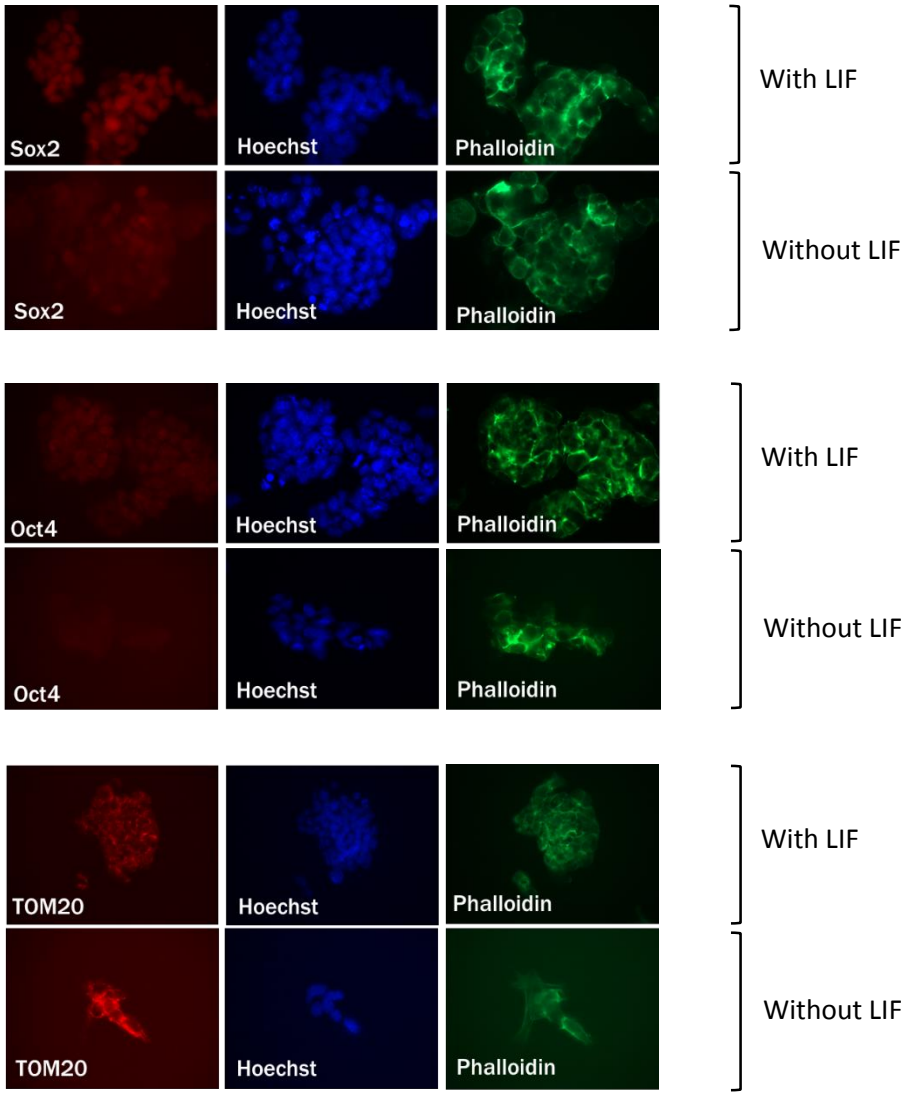

Figure 14 - Immunocytochemistry for Oct4 and Sox2 (pluripotency markers) and TOM20 (mitochondrial marker), with and without LIF. Phalloidin (actin-binding probe) and Hoecsht (DNA binding dye) staining allow co-localization all three proteins. 63x magnification.

Both SOX2 and OCT4 staining seem to be higher in cells cultured with LIF-supplemented medium, which suggests they could be labeled as having a more pluripotent phenotype than those in the second row, which were cultivated in medium without LIF. This result supports the theory that the morphology of mESC colonies is a fairly good indicator of the "stemness" of these E14 cells.

Along with transcription factors, immunocytochemistry was also performed against TOM20, a mitochondrial surface protein, commonly used as a measure of total mitochondrial mass and cell localization. These results suggest that mESC possess a diminished mitochondrial mass, which increases with differentiation.

Besides the use of antibodies for the aforementioned pluripotency markers, two molecular probes for actin (phalloidin) and the nucleus (Hoecsht), which were meant to

provide structural context and, in a way, co-localize the proteins assayed. In this case, both SOX2 and OCT4 co-localize with Hoechst, indicating their nuclear localization, while TOM20 is located in the cytoplasm, as expected, through its co-localization with phalloidin.

Being able to both culture and handle ESC, we then proceeded to perform differentiation protocols for these cells, to further characterize their stem profile.

4.1.2 Differentiation of mESC

4.1.2.1 Embryoid Body differentiation

ESC are able to differentiate into the three germ layers (endoderm, mesoderm and ectoderm). While some (metabolic) modulators may affect the pluripotent phenotype of ESCs, some of them only reveal modulating action when cells start to differentiate. Therefore, an established protocol for ESC differentiation is required, if the mechanisms of said modulators are to be assayed.

In vitro, the differentiation process can be either directed towards a (rather) specific cell type or tissue, or it may be unspecific, generating embryoid bodies (EBs). EBs consists of disordered, differentiated tissue, presenting a heterogeneous mixture of cell types. In order to achieve both directed and undirected differentiation, the first step requires for an exchange of medium, abandoning the use of a pluripotency-inducing medium. In the case of the undirected differentiation, the difference resides in ceasing to supplement the KODMEM culture medium with LIF, and plating cells considerably more densely in non-adherent cell culture dishes to let them to aggregate and then, at day three putting them in normal growth dishes coated with gelatin.

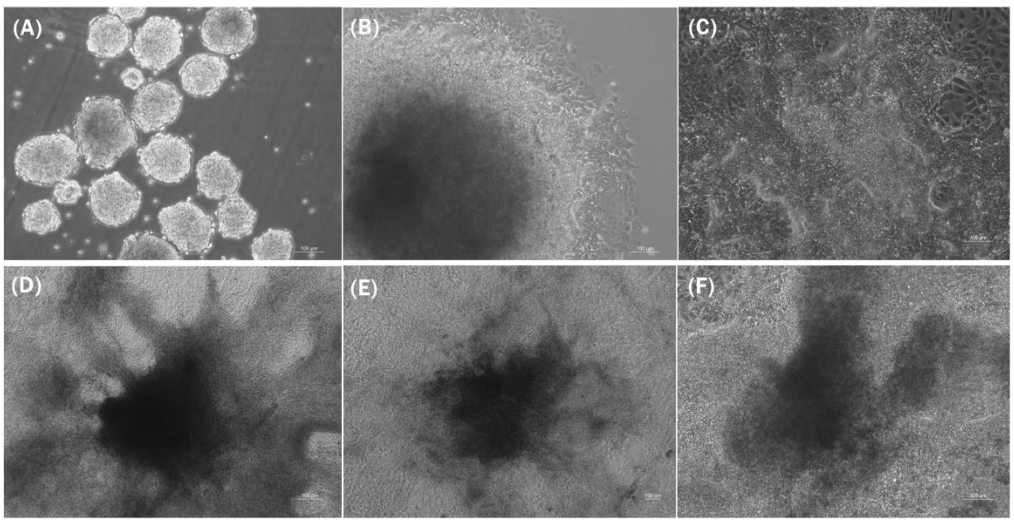

Figure 15 - Embroyd body differentiation through days 2, still in suspension (A); 4, adhered 1 day (B); 7, adhered 4 days (C); 9, adhered 6 days (D); 11, adhered 8 days (E); and adhered for 11 days 14 (F). Scale bar is 100 µm.

Throughout the 14 day differentiation protocol, increasingly complex structures assemble, the three-dimensional organization becoming obvious after day 7, with the existence of two or more focal points in microscopy imaging, which is an indication of different heights in the colonies, as evident in Figure 15 (as some of the cells in culture seem unfocused in these photographs). In the later days of differentiation, the cores of these megastructures appear as black or brown, a possible indicator of necrosis/apoptosis. Due to the sheer cell density in this culture type, the nutrient demands require daily media exchange.

As stated, this differentiation process gives rise to precursors of all three germ layers, and whole-protein lysates reveal the expression of differentiation marks for those germ layers, with a concomitant decrease of the expression of pluripotency markers. So, in order to prove the "stemness" of these cells, western blot for different both pluripotency and differentiation markers was performed, and the expression of these markers, quantified. The next figures refer to an Embryoid Bodies differentiation, over 14 days, while collecting the total protein content every two days (starting from day 2 after plating).

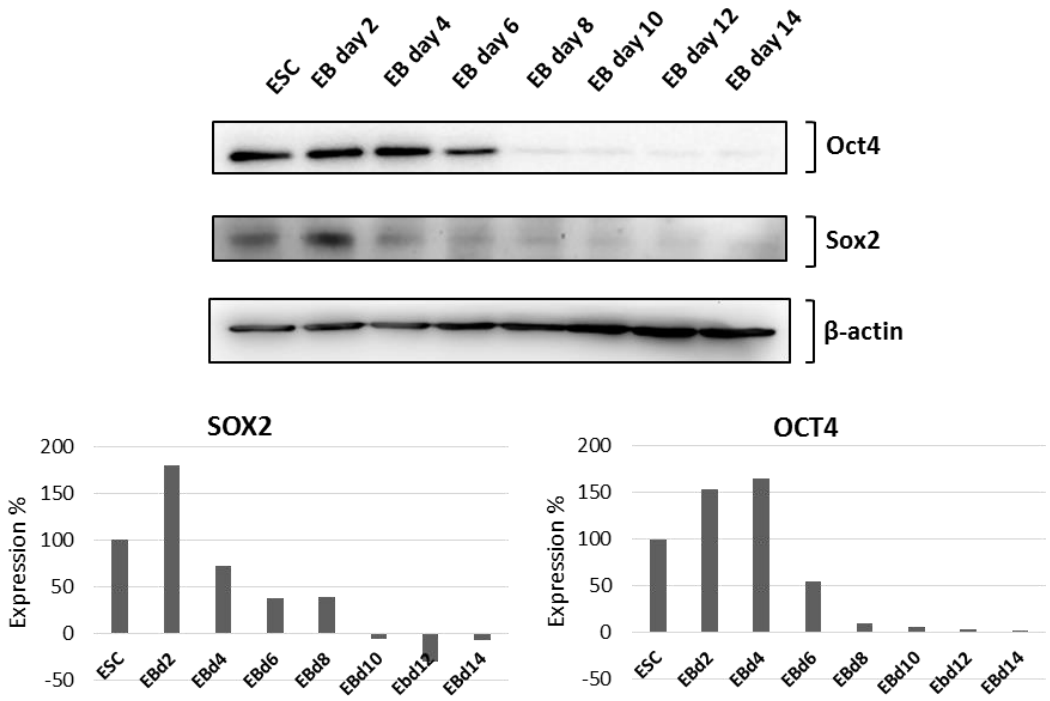

Figure 16 - Western Blotting for Pluripotency Markers for E14 ESC and EBs. These blot images and respective quantifications are the result of one experiment.

Pluripotency was measured by the expression of different pluripotency markers. In Figure 16, some of these markers can be observed, and their expression lowers throughout the differentiation process. This is obvious for OCT4 and SOX2 two of the "core" pluripotency potency markers (the others are KLF4 and NANOG). These four pluripotency markers are transcription factors, which were found to be highly expressed in the first stages of murine embryonic development(Zhao et al., 2012).

This steady decrease shows that loss of pluripotency is a gradual process and that cells do not immediately start to lose pluripotency after ceasing to be cultured in pluripotency-sustaining conditions.

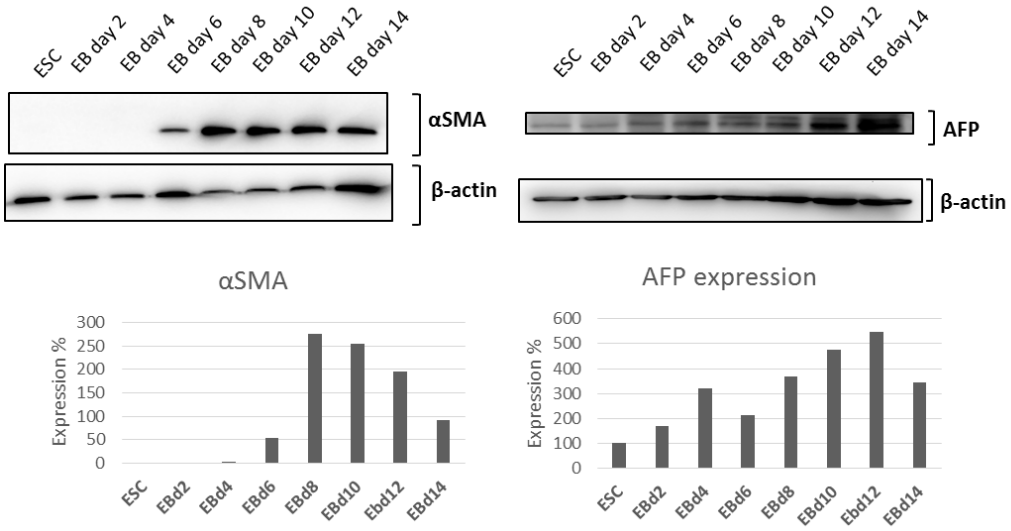

Figure 17 - Western Blotting for Differentiation Markers for E14 ESC and EBs. Resulting quantifications are the result of one experiment each.

Along with a progressive loss of pluripotency, cells differentiating in this way will show increasing levels of specific markers for specific tissues. Therefore, to further characterize these differentiating culture, western blotting for markers of primordial germ layers. Figure 17 shows that overtime, markers for all two germ layers (AFP for primordial endoderm(Abe et al., 1996), αSMA for mesoderm (Skalli et al., 1989)) are increasing somewhat steadily. The different expression rates (in cases, decreasing, as seen for the levels of αSMA) may not refer to a lesser increase of that specific cell type, but that its increase may be lessened when compared with other cell types: seeing as this quantification is normalized to β-actin, that is a measure of total protein mass, there could be more cells contributing to the whole protein content, but not specifically expressing one cell marker. Case in point, and while not evident because of the very different scale, it appears that AFP-positive cells show an approximate enrichment of 400% on day six, having increased through the whole assayed period in a stable manner, greatly outmatching the apparent enrichment of αSMA–positive cells. In order to fully understand and measure the true enrichment for each germ layer, flow-cytometry could be performed. But as the purpose of the aforementioned assay was to show the differentiation capabilities of E14 cells, the WB analysis clearly showed that capability.

A similar assay should have been performed to characterize the capability of these cells to commit to a neuronal lineage, but the antibody did not work for western blot. Nonetheless, these cells are able to generate neuronal germ line, as shown in Figure 21.

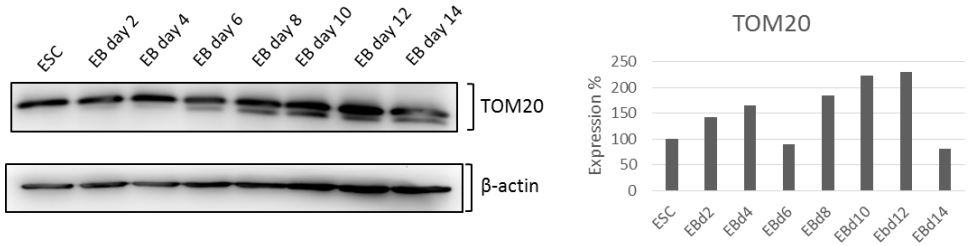

Figure 18 - Western Blot image and quantification for TOM20, a mitochondrial mass indicator.

It has been shown before that along with differentiation comes an increase in the mitochondrial mass, cause and consequence of an increased mitochondrial metabolism and general activity(Cho et al., 2006; Facucho-Oliveira and St John, 2009; Facucho-Oliveira et al., 2007). With this in mind, a western blot against TOM20, an outer mitochondrial membrane protein, which would provide a measure of mitochondrial mass, was performed, and the corresponding results can be seen in Figure 18. There is a trending increase in the expression of this protein, as expected. Nonetheless, this crude measure doesn't possess the means to hint an increased mitochondrial function. Noticing the sudden decrease in the quantification graph, referring to the last differentiation day in the expression of TOM20, it is due to the slight overexposure of the western blot membrane during the image acquisition process. As it is visible in the blot image, the band of immunostained TOM20 is considerably larger than the preceding band (day 12), and therefore, should mean that indeed, the increase of TOM20's expression throughout the differentiation period is steadily increasing.

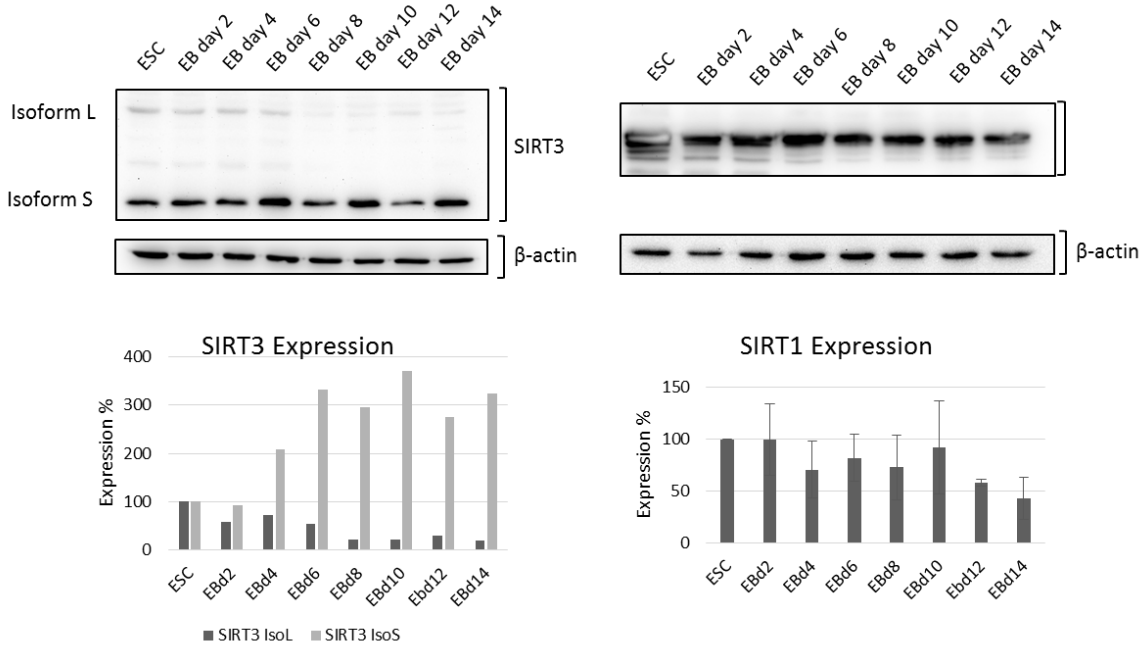

Figure 19 - Western Blot images and quantification of the primary mitochondrial sirtuin (SIRT3) and the most studied sirtuin, SIRT1. Quantifications are the result of two independent experiments.

Having characterized the differentiation of mESC, we then shifted our attention to the expression of both SIRT1 and SIRT3 along the differentiation process. It has been reported that mESC have increased expression of SIRT1 when compared with more differentiated cells (Saunders et al., 2010), and is vital for normal embryonic development (Cheng et al., 2003). The data in Figure 19 appear to support the former, as the expression of SIRT1 during the assayed period steadily drops. The measurement of SIRT1 were meant to, in part, further characterize the differentiation of E14 in Embryoid Bodies, but also to support the study of eventual influence of SIRT3 KD in the levels of other sirtuins (namely, SIRT1) during differentiation.

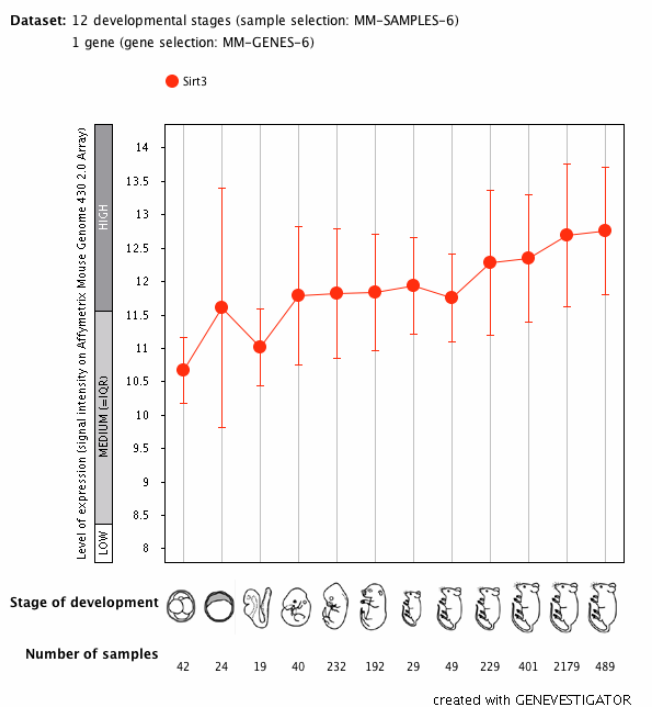

Figure 20 – Microarray data analysis for the expression for Sirt3 mRNA during different stages of mouse embryonic development. Acquired from GENEVESTIGATOR (7th of July, 2015).

On the other hand, the expression of SIRT3 seems to increase during differentiation, as seen in Figure 19, which supports the notion that SIRT3 is involved in the activation of the mitochondria's metabolism and activity, which has in turn been reported to increase as ESC differentiate(Abdel Khalek et al., 2014; Kawamura and Uchijima, 2010; Rodriguez et al., 2013; Wang et al., 2014). This increase is also supported by already reported data, although referring to mRNA, as shown in Figure 20. As it has been reported that the inhibition of mitochondrial metabolism could compromise mESC differentiation (Pereira et al., 2013), mitigating the effects of SIRT3 through silencing could present a similar effect.

4.1.2.2 Neuronal Differentiation

To differentiate stem cells in a more or less specific cell type, which is to say, generate a less heterogeneous culture, a more chemically defined medium, with specific supplements, is required. Neuron progenitors were differentiated from E14 cells and immunostained for β-III Tubulin after 14 days off neuronal differentiation. Cells were also incubated with Hoescht 33342, a DNA-binding probe, which allowed staining of the nucleus. The resulting images, are shown in Figure 21, along with the correspondent phase contrast microphotographs.

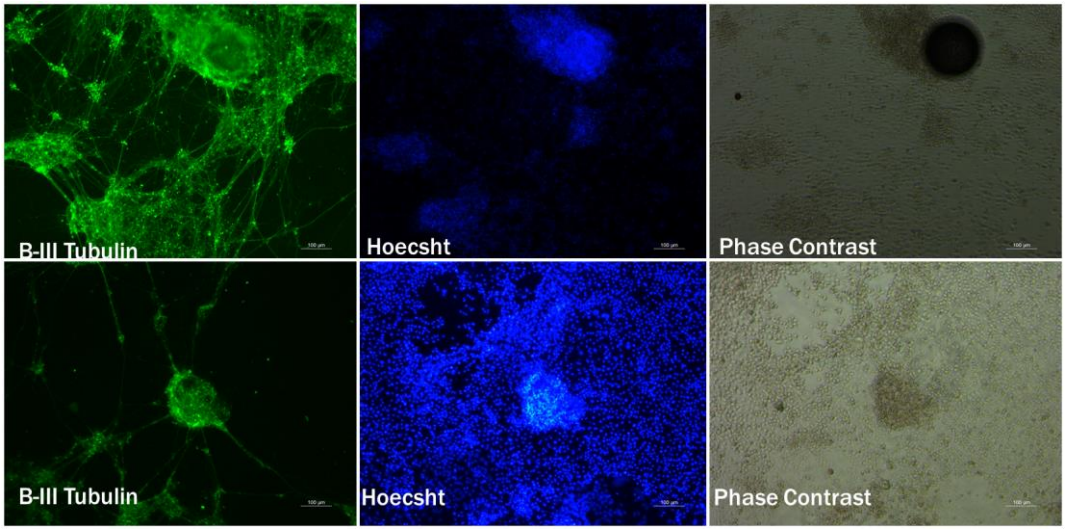

Figure 21 - Neuronal-directed differentiation of E14 mESC. Immunocytochemistry for B-III Tubulin (pan neuronal marker).

4.2 Molecular Biology: Plasmid Characterization, Bacterial Culture and DNA amplification/Isolation

4.2.1 Plasmid elements and description

A

```
1 acttccgcta aacttctccc gggtttctgg ccctgccctt gaggcattaa agagtagagg
61 tgcctggggа cagctagcca ctgactggtc acgtagcctc aagcctgcag acttgggtcc
121 tctgaaaccg gatggcgttt ggcgaggact agtgttacag gtgggagaag gcccatatcc
181 ctctgtgtgg gagcctcagg cggctttgga ggtggaggaa gcagtgagaa gaagttttct
241 ctgcaggatg tagctgagct gcttcggacc agagcctgca gtagggtggt ggtcatggtg
301 ggggccggca tcagcacacc cagtggcatc ccggacttca gatccccagg gagcggcctc
361 tacagcaacc ttcagcagta tgacatcccg taccctgaag ccatctttga acttggcttt
421 ttctttcaca accccaagcc ctttttcatg ttggccaagg agctgtaccc tgggcactac
481 aggcccaatg tcactcacta cttcctgagg ctcctccacg acaaggagct gcttctgcgg
541 ctctatacac agaacatcga cgggcttgag agagcatctg ggatccctgc ctcaaagctg
601 gttgaagccc acgggacctt tgtaacagct acatgcacgg tctgtcgaag gtccttccca
661 ggggaagaca tatgggctga tgtgatggcg gacagggtgc ccgctgccc tgtctgtact
721 ggcgttgtga aacccgacat tgtgttcttt ggggagcagc tgcctgcaag gttcctactc
781 catatggctg acttcgcttt ggcagatctg ctactcattc ttgggacctc cctggaggtg
841 gagccttttg ccagcttgtc tgaagcagta cagaaatcag tgcccgact gctcatcaat
901 cgagacttgg tggggccgtt cgttctgagt cctcgaagga aagatgtggt ccagctaggg
961 gatgtagttc atggtgtgga aaggctggtg gacctcctgg ggtggacaca agaactgctg
1021 gatcttatgc agcgggaacg tggcaagctg gatggacagg acagataaga ctatggcttc
1081 ttcacctggg gaagtcacac agcagatcat cctatgtcca gcaagacttc atgcctgaag
1141 acagctccaa cacgtttaca aacatgaacc agaccacaac atgtggcctg gacagtggtc
1201 ctccgaggct gcctttggaa aggctgacca gggatgtcta cccttggggc ccctccatgt
1261 gtgcgccctg tccacctcat cactgctgaa ggtgtagtgc aggtgctgct ttctgcagcg
1321 gcccttaagt tatcacgagg gcagcacagc acgcccgtcg ccaggcaggc gatgcactag
1381 ggcaatctag catgttgatc ggtaaagtgg catctttaac tacaacatca tttcttgcat
1441 gaaataaact tagtataaaa acttggcaaa aaaaaaaaaa aaaa
```

B

```
1 ggggattcgg atggcgcttg accctctagg cgccgtcgtc ctgcagagca tcatggcgct
61 aagcggtcga ctggcattgg ccgcgctcag actgtggggt ccgggagtgt tacaggtggg
121 agaaggccca tatccctctg tgtgggagcc tcaggcggct ttggaggtgg aggaagcagt
181 gagaagaagt tttctctgca ggatgtagct gagctgcttc ggaccagagc ctgcagtagg
241 gtggtggtca tggtgggggc cggcatcagc acacccagtg gcatcccgga cttcagatcc
301 ccagggagcg gcctctacag caaccttcag cagtatgaca tcccgtaccc tgaagccatc
361 tttgaacttg gctttttctt tcacaacccc aagccctttt tcatgttggc caaggagctg
421 taccctgggc actacaggcc caatgtcact cactacttcc tgaggctcct ccacgacaag
481 gagctgcttc tgcggctcta tacacagaac atcgacgggc ttgagagagc atctgggatc
541 cctgcctcaa agctggttga agcccacggg acctttgtaa cagctacatg cacggtctgt
601 cgaaggtcct tcccagggga agacatatgg gctgatgtga tggcggacag ggtgccccgc
661 tgccctgtct gtactggcgt tgtgaaaccc gacattgtgt tctttgggga gcagctgcct
721 gcaaggttcc tactccatat ggctgacttc gctttggcag atctgctact cattcttggg
781 acctccctgg aggtggagcc ttttgccagc ttgtctgaag cagtacagaa atcagtgccc
841 cgactgctca tcaatcgaga cttggtgggg ccgttcgttc tgagtcctcg aaggaaagat
901 gtggtccagc taggggatgt agttcatggt gtggaaaggc tggtggacct cctggggtgg
961 acacaagaac tgctggatct tatgcagcgg gaacgtggca agctggatgg acaggacaga
1021 taagactatg gcttcttcac ctggggaagt cacacagcag atcatcctat gtccagcaag
1081 acttcatgcc tgaagacagc tccaacacgt ttacaaacat gaaccagacc acaacatgtg
1141 gcctggacag tggtcctccg aggctgcctt tggaaaggct gaccagggat gtctaccctt
1201 ggggcccctc catgtgtgcg ccctgtccac ctcatcactg ctgaaggtgt agtgcaggtg
1261 ctgctttctg cagcggccct taagttatca cgagggcagc acagcacgcc cgtcgccagg
1321 caggcgatgc actagggcaa tctagcatgt tgatcggtaa agtggcatct ttaactacaa
1381 catcatttct tgcatgaaat aaacttagta taaaaacttg gcaaaaaaaa aaaaaaaaa
```

C

```
1 ggggattcgg atggcgcttg accctctagg cgccgtcgtc ctgcagagca tcatggcgct
61 aagcggtcga ctggcattgg ccgcgctcag actgtggggt ccgggaggtg ggagaaggcc
121 catatccctc tgtgtgggag cctcaggcgg ctttggaggt ggaggaagca gtgagaagaa
181 gttttctctg caggatgtag ctgagctgct tcggaccaga gcctgcagta gggtggtggt
241 catggtgggg gccggcatca gcacacccag tggcatcccg gacttcagat ccccagggag
301 cggcctctac agcaaccttc agcagtatga catcccgtac cctgaagcca tctttgaact
361 tggctttttc tttcacaacc ccaagccctt tttcatgttg gccaaggagc tgtaccctgg
421 gcactacagg cccaatgtca ctcactactt cctgaggctc ctccacgaca aggagctgct
481 tctgcggctc tatacacaga acatcgacgg gcttgagaga gcatctggga tccctgcctc
541 aaagctggtt gaagcccacg ggacctttgt aacagctaca tgcacggtct gtcgaaggtc
601 cttcccaggg gaagacatat gggctgatgt gatggcggac agggtgcccc gctgccctgt
661 ctgtactggc gttgtgaaac ccgacattgt gttctttggg gagcagctgc ctgcaaggtt
721 cctactccat atggctgact tcgctttggc agatctgcta ctcattcttg ggacctccct
781 ggaggtggag ccttttgcca gcttgtctga agcagtacag aaatcagtgc cccgactgct
841 catcaatcga gacttggtgg ggccgttcgt tctgagtcct cgaaggaaag atgtggtcca
901 gctaggggat gtagttcatg gtgtggaaag gctggtggac ctcctggggt ggacacaaga
961 actgctggat cttatgcagc gggaacgtgg caagctggat ggacaggaca gataagacta
1021 tggcttcttc acctggggaa gtcacacagc agatcatcct atgtccagca agacttcatg
1081 cctgaag aca gctccaacac gtttac aaac atgaaccaga ccacaacatg tggcctggac
1141 agtggtcctc cgaggctgcc tttggaaagg ctgaccaggg atgtctaccc ttggggcccc
1201 tccatgtgtg cgccctgtcc acctcatcac tgctgaaggt gtagtgcagg tgctgctttc
1261 tgcagcggcc cttaagttat cacgagggca gcacagcacg cccgtcgcca ggcaggcgat
1321 gcactagggc aatctagcat gttgatcggt aaagtggcat ctttaactac aacatcattt
1381 cttgcatgaa ataaacttag tataaaaact tggcaaaaaa aaaaaaaaaa a
```

D

scr - GCTTCGCGCCGTAGTCCTA
sh1- CGGCTCTATACACAGAACA
sh2- TGCAAGGTTCCTACTCCAT
sh3- GACTGCTCATCAATCGAGA
sh4- ACAGCTCCAACACGTTTAC

E

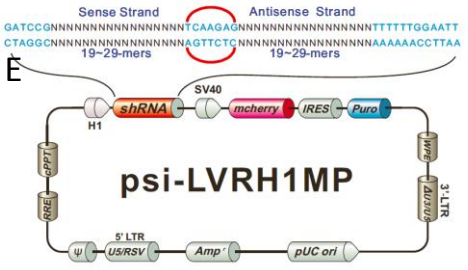

Figure 22 – mRNA sequences for the three main alternative splicings for Sirtuin3, with the shRNA targets highlighted. A – mRNA sequence for the SIRT3 transcript variant 1, regarded as cytoplasmic. B - mRNA sequence for the SIRT3 transcript variant 2, regarded as cytoplasmic. C - mRNA sequence for the SIRT3 transcript variant 3, regarded mitochondrial. D – mRNA target sequences for plasmid-expressed shRNAs. E – shRNA-expressing plasmid chosen for transfection.

The first step we must take when aiming to perform a protein knockdown is to have knowledge of the target protein's mRNA sequence, in order to design short nucleotide sequences that will later be used by the cell's enzymatic silencing machinery, as described before. These short sequences, typically of 19 to 30 nucleotides should be specific to the target sequence and, very much like primer designing, shouldn't align with other sequences. In Figure 22, the canonical mRNA sequences for SIRT3 are shown, where sequences A and C give rise to the shorter isoform of SIRT3 (Isoform S, 28kDa), which is regarded as cytoplasmic and not possessing relevant deacetylating activity. The remaining sequence (B) may equally code for the three isoforms of SIRT3, and therefore, a longer isoform (Isoform L, 36kDa), will surely

derived from this sequence(Yang et al., 2010). Yang and colleagues demonstrated the differential expression of SIRT3's isoforms, and also established their localization and activity, which have been previously hinted by others (Bao et al., 2010; Cooper et al., 2009; Shi et al., 2005). As we were interested in the mitochondrial portion of the cell metabolism, and SIRT3 is documented to mainly deacetylate mitochondrial proteins, we will focus on SIRT3 Isoform L (Sirt3-L).

Many knockdown solutions are commercially available, depending on the specific silencing one wishes to achieve. siRNAs can be directly transfected and very transiently knockdown a target protein. Viral vectors allow for the chromosomal integration of shRNA expressing DNA sequences, generating a genetic, stable, knockdown. Or, if a balanced solution is sought, plasmids expressing those shRNAs are perhaps the most adequate choice. The advantage of using this type of construct, along with increased stability, is that other elements can be included in the same plasmid, such as reporter proteins and/or selection markers. The first allows the user to quickly identify if the transfection was successful, and the second provides a way to obtain a more or less homogeneously transfected culture.

Therefore, we for a plasmid construct that would provide all the elements described. Among many suppliers, the best plasmid choices were given by Genecopeia™, which allowed us to choose the target protein, selection marker and the reporter gene. Figure 22E shows the chosen plasmid for transfection. It includes the fluorescent reporter protein mCherry (allows us to fluorescently track the transfection status of cultured cells), and also a selection marker (a puromycin resistance gene). The plasmid also includes two "strong" promoters, H1 (histone1) and SV40 (Simian vacuolating virus 40), to assure extensive expression of both the shRNA and annex components of the plasmid. 4 plasmids expressing shRNA for 4 different regions of SIRT3 mRNA and one plasmid encodes for a "mock" shRNA (shRNAscr, which does not recognize none of the presented sequences. This plasmid, therefore, is meant to show that the decrease in SIRT3 is due to the shRNA sequences present, and not to the plasmid itself. The sequences targeted by each shRNA in mRNA of SIRT3 are highlighted, and each color corresponds to a different shRNA-targeting sequence. BLAST analysis for both the shRNAscr and each individual shRNA (1-4), showed that a) the target sequence for the shRNAscr has a low sequence alignment score for *mus musculus* transcripts, and b) shRNA (1-4) have maximum sequence alignment score to the aforementioned SIRT3 mRNA sequences, and a low score for every other mRNA sequence in *Mus musculus* transcripts.

It should be noted that this plasmid also incorporates elements that allow it to be integrated in a host genome if lentiviral vectors were to be used. These elements (5' and 3' LTR and Psi (Ψ)) are used by retroviruses to integrate their genetic information on the host genome, allowing the virus to replicate.(Klimo et al., 2004; Xu, 2011).

4.2.2 Bacterial transformation

After choosing the plasmid that will be employed to transfect and silence SIRT3 in mammalian cell lines, we proceeded to transform *E.coli* in order to amplify the initial amount

of DNA. This would allow me to have a steady stock of plasmidic DNA for each shRNA, without needing to continuously order new plasmids. As the chosen plasmid contains, among other elements, a prokaryote origin of replication (pUC ori), it allows for this type of procedure. After transformed with each shRNA-expressing plasmid (separately) through heat-shock, bacteria were plated in different LB-agar plates, as shown in Figure 23, and incubated overnight. To assure both the sterility of our work, and the stability of the antibiotics in the LB-agar plates, adequate controls were used. Therefore, WT (non-transformed *E.coli,* putatively sensitive to carbenicillin) were plated in LB-agar plates with and without antibiotic, as presented in Figure 23A and Figure 23B. As they are not resistant to carbenicillin, WT *E.coli* does not proliferate, as seen in LB-agar without addition of any antibiotic. Nevertheless, plasmid positive *E.coli* colonies are seen throughout Figure 23C to Figure 23H, as they are resistant to carbenicillin, the resistance being conferred by the shRNA-expressing plasmid. Before following up to plasmid DNA isolation, these colonies must be visually analyzed, and only *E.coli* colonies without satellite colonies (indicators of antibiotic depletion) were picked and cultured in SOC medium to increase the plasmid-containing bacterial mass.

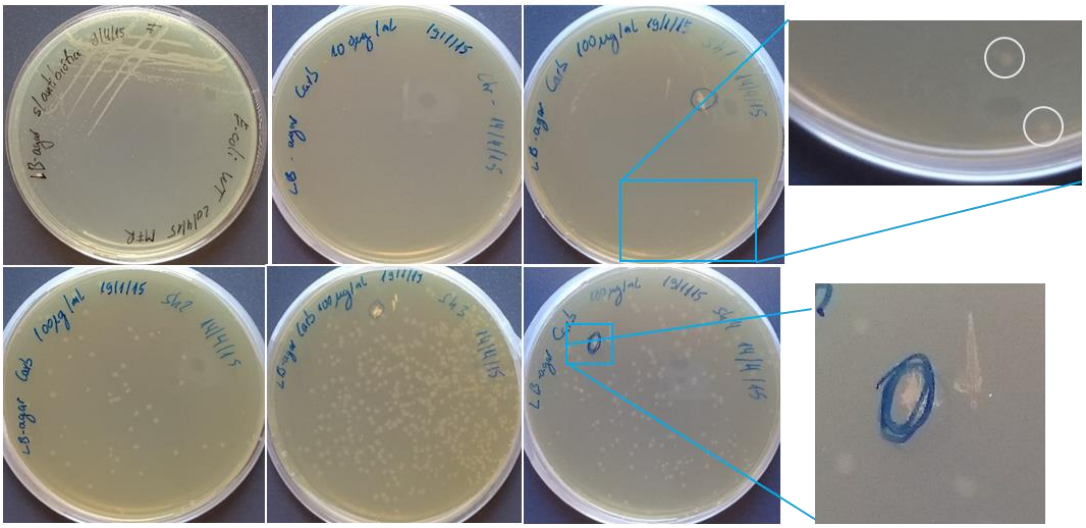

Figure 23 -Transformed E.coli in LB-agar plates, after overnight incubation. A - Bacterial streaking of WT E.coli in LB-agar plate. B -Bacterial streaking of WT E.coli in LB-agar plate with 50ug/mL carbenicillin antibiotic. C – LB-agar plate with 50ug/mL carbenicillin, plated with shRNA1 transformed E.coli. D –Zoomed section of plate C, with two plasmid-positive E.coli colonies, ready to be picked to the DNA isolation process. E - LB-agar plate with 50ug/mL carbenicillin, plated with shRNA2 transformed E.coli. F - LB-agar plate with 50ug/mL carbenicillin, plated with shRNA3 transformed E.coli. G - LB-agar plate with 50ug/mL carbenicillin, plated with shRNA4 transformed E.coli. H - Zoomed section of plate C, with an already picked plasmid-positive colony circled in blue ink.

To achieve an initial mass of plasmid positive bacteria large enough to assure a profitable amount of amplified plasmid DNA, two SOC broth cultures were performed. This broth is somewhat similar to LB broth, while differing in cation presence (increased Ca^{2+} and Mg^{2+}) and also increased glucose content, important for catabolite repression, which, in short, allows bacteria to adapt and have increased growth rate. The choice of this medium over LB was due to it being reported to increase the efficiency of bacterial transformation (Hanahan, 1983).

An overnight culture starting with a single colony, picked as described above, and inoculated in a typical volume of 5 mL, with 50ug/mL carbenicillin. Again, to assure the sterility

of the process and the stability of the components, three controls were performed, as shown in Figure 24. WT *E.coli* were picked from the corresponding LB-agar plate (shown above) in SOC broth with and without antibiotic (Figure 24A and D), proving that the antibiotic is still selecting bacteria based on the plasmid presence (or rather absence). Another experiment, meant to show that in fact, antibiotic resistance conferred by the shRNA-expressing plasmid is specific for carbenicillin was conducted, by inoculating shRNA-expressing plasmid colonies in SOC broth with added kanamycin (100ug/mL). As seen in Figure 24C, by the lack of turbidity of the medium, transformed *E.coli* aren't able to grow.

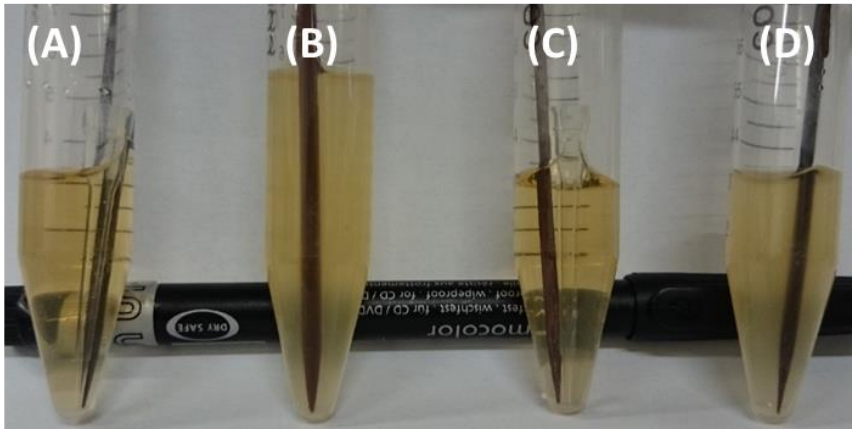

Figure 24 – SOC cultures of both WT and transformed E.coli, *after 8 hours of incubation at 37°C with agitation. Turbidity indicates bacterial growth. (A) - WT E.coli + SOC broth + 50ug/mL carbenicillin. B – Plasmid positive E.coli + SOC broth + 50ug/mL carbenicillin. C – Plasmid positive E.coli + SOC broth + 100ug/mL kanamycin. D - WT E.coli + SOC broth.*

In the following morning, these containers are observed to confirm bacterial growth (visible turbidity), and then prepared to undergo the DNA extraction/isolation process.

4.2.3 DNA isolation, quantification, characterization

Nowadays DNA isolation is usually performed with premade kits that rely in chromatographic isolation of DNA, with adequate chromatographic columns. Various kits are commercially available, the distinguishing attribute being mainly the bacterial culture volume that we want to start from. As we were unsure of the efficiency of our transformation protocol, we started by ordering a smaller kit (dubbed "Miniprep", short for minipreparation, a fast and small-scaled isolation process), starting with bacterial cultures up to 5 mL. After conducting the aforementioned process, we proceeded to quantify the DNA isolates (as seen in Figure 25). We also electrophorectically confirmed the plasmid size through a 1% agarose gel, which showed well-defined bands of approximately 8500 bp, as expected.

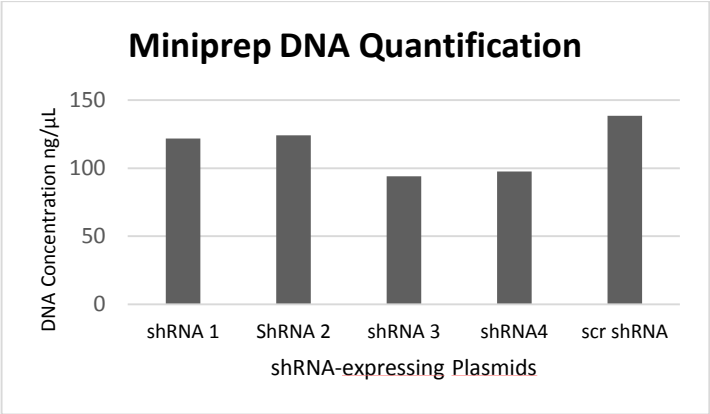

Figure 25 - Quantification of shRNA-expressing plasmids isolated from E.coli *through the Miniprep kit.*

Having both our transformation and bacterial growth protocols validated, and having an increased pool of plasmid DNA to work with (so we could save the ordered aliquots of both consumption and freeze-thaw-derived degradation), we scaled up the process, to increase the yield of plasmid DNA. Therefore, we tested the DNA yield of a Maxiprep kit, which required at least 200 mL of bacterial culture. This large culture required a pre-culture of picked *E.coli*.

After the "overday" incubation of picked colonies, very much alike the one shown in Figure 24, a scaled up culture is prepared. The contents of the shRNA-expressing plasmid-positive colonies were transferred to a 1L Erlenmeyer flask with 300 mL of SOC broth with 50µg/mL carbenicillin, labelled, and incubated overnight at 37°C with agitation.

In the morning following this incubation period, the Maxiprep kit for DNA isolation is used according to the manufacturer's instructions. The isolated DNA is then precipitated with isopropanol, and "cleaned" with ethanol before being diluted in water. This water-diluted DNA is, like before, characterized by quantification and agarose electrophoresis, the resulting images visible in Figure 26. The plasmid DNA isolates were aliquoted and frozen, pending transfection.

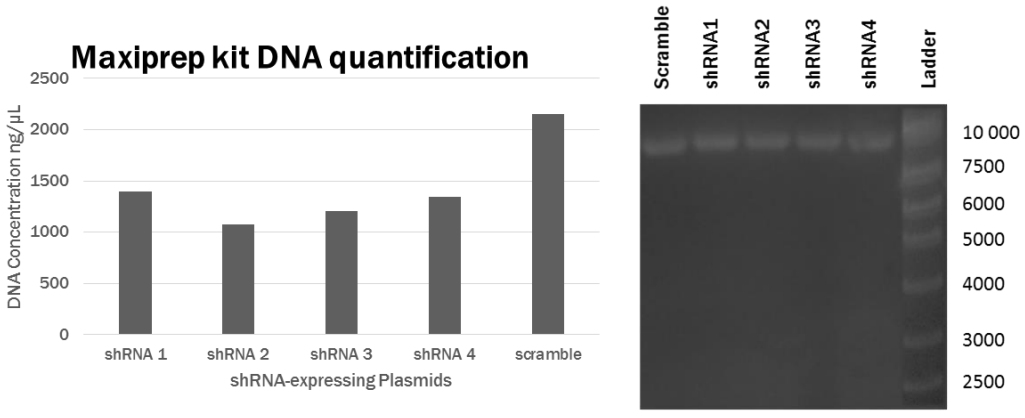

Figure 26 - Characterization of shRNA expressing plasmids isolated via the Maxiprep kit. A - Quantification of plasmid DNA for each isolate. B - Agarose gel electrophoresis for plasmid DNA, along with a DNA ladder.

In addition to the plasmid size and concentration, another factor we took into consideration in order to further characterize the DNA isolates were the absorvance ratios for each samples. During the quantification process by the *Nanodrop®* apparatus, two absorbance ratios are obtained, as seen in Table 8. These ratios reflect the purity of the DNA sample, regarding both protein contamination (proteins absorb mainly at 280nm, while double-stranded DNA absorbs at 260 nm), but also contamination with organic reagents, often used during the isolation of nucleic acids (some of these reagents, like TRIzol, absorb primarily at 230nm). Therefore, relatively high values for both absorbance ratios is a good indicator of DNA purity. The values for both absorbance ratios, for all the assayed samples, are higher than those regarded as the "minimum optimal values" by the manufacturer (Thermo Scientific, 2011), and so, we consider that our samples are pure, and were rather satisfied with the new DNA pool and turned to this kit whenever new DNA samples were required.

Table 8 - DNA quantification for Maxiprep kit isolates. Quantification was performed in a Nanodrop® apparatus.

shRNA-expressing plasmid	*Concentration (ng/µL)*	*Absorbance Ratios*	
		260/280	260/230
shRNA 1	1400.1	2.01	2,44
shRNA 2	1072.7	1.99	2,39
shRNA 3	1207	1.98	2,38
shRNA 4	1347.5	2.02	2,42
Scrambled shRNA	2152	1.93	2,38

4.3 SIRT3 SILENCING IN MESC

4.3.1 mESC selection conditions (SRB and cell counting)

After cell transfection, the plasmid-positive cells must be selected, so that the most homogeneous culture of positively transfected cells can be achieved. As explained above, the chosen plasmid contains a gene that gives resistance to puromycin in mammalian cells. This allows us to use the antibiotic puromycin to select the plasmid-positive cells, while killing all other, non-transfected cells. Therefore, we must determine beforehand which amount of puromycin is enough to eliminate all cells without the resistance-conferring gene: unstransfected cells are plated, and then, different concentrations of puromycin are added in the following day. Media was exchanged daily until day 7, when the highest of puromycin was able to eliminate every cell in culture. After, the surviving cell number and total cell density was assayed, in order to select the adequate puromycin concentration.

This procedure was conducted for E14 mESCs, and the results for both cell counting and cell density (attained through SRB) is seen in Figure 27. We have chosen 1µg/mL puromycin as an adequate concentration to select puromycin-resistant cells, once it was the lowest tested concentration of puromycin that was able to eliminate all cultured cells.

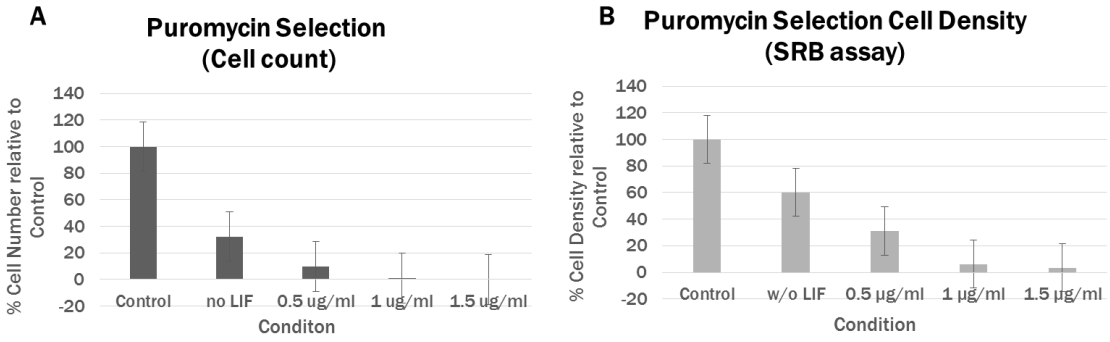

Figure 27 - Selection conditions for transfected E14 cells. Cells were either manually counted (A) or subject to sulforhodamine B (B). These results were obtained from three independent experiments.

4.3.2 Transfection protocol and optimization (DNA:Lipofectamine ratios, incubation times)

Having prepared all the elements required to achieve transfection in mESC, the first step of the process was to assay for the eventual toxicity of Lipofectamine® 2000 in these cells. As seen in Figure 28, there was no apparent toxic effect of lipofectamine on the cultured cells. The amount of both OptiMEM and Lipofectamine® 2000 added was concomitant with those employed in the following transfections with shRNA-expressing plasmids.

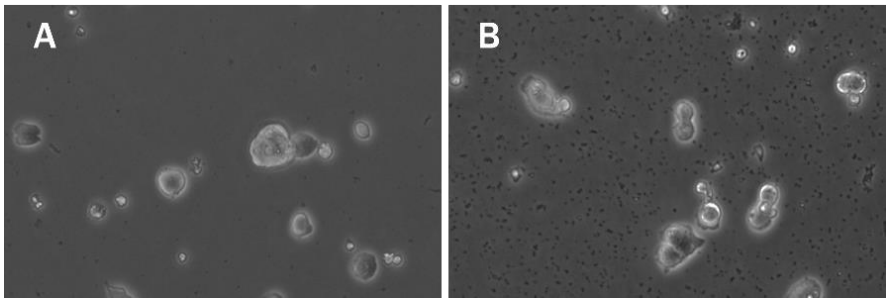

Figure 28 - Microscopy imaging for E14 cells 24 hours after plating with (A) OptiMEM and (B) OptiMEM with Lipofectamine®2000

The next step in transfecting mESC and optimizing the transfection protocol was to use different Lipofectamine:DNA ratios, as it has been reported that these ratios may influence the transfection efficiency(Maurisse et al., 2010). This lead us to, based on literature, select a total of 4 DNA:Lipofectamine® 2000 ratios (DNA:Lipofectamine®2000 1:1, 1:2, 1:3 and 1:4 ratio), preparing the transfections accordingly, and evaluating the transfection efficiency after the application of the protocol. Without any antibiotic selection, the cells were observed with fluorescence microscopy 48 hours after transfection, as shown in Figure 29.

Increasing concentrations of Lipofectamine® seem to increase the total number of mCherry-fluorescent cells, even when comparing with the total cell number as visible in phase contrast images. Based in these results, subsequent transfections were performed using a 1:4 ratio for DNA:Lipofectamine® 2000.

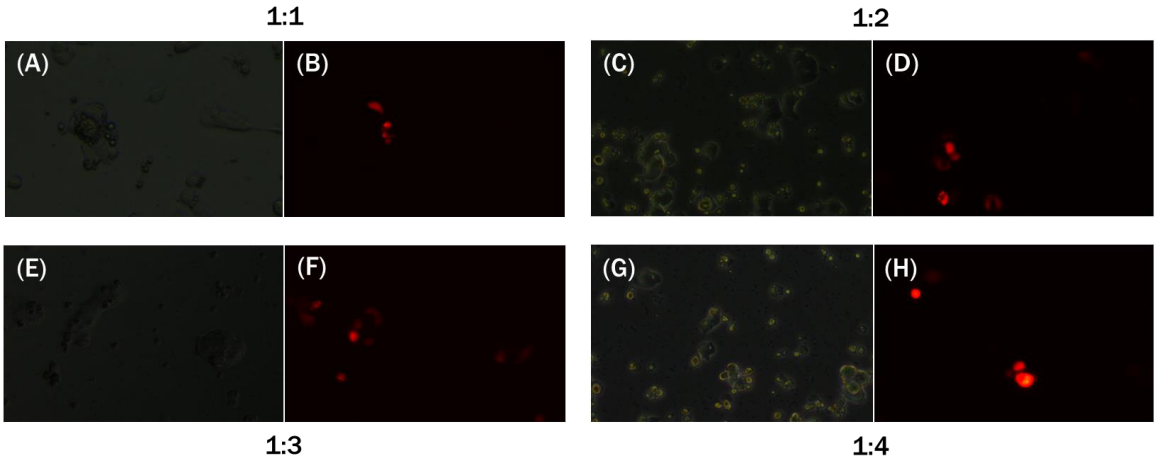

Figure 29 - Representative images of E14 mESC transfected with different Lipofectamine®2000:DNA ratios, with the DNA:Lipofectamine 3000 ratios adjacent. A, C, E and G represent phase contrast images, while B, D, F and H represent fluorescence images. Scale bar is 100µm.

While we understand, to some extent, that the transfection had been successful, as the plasmid entered the cells, and its reporter gene (mCherry) is being expressed, the ratio of transfected/non-transfected cells was low, revealing that the process was inefficient. As it was been reported that Lipofectamine® 3000 would yield better transfection rates, we repeated the protocol while using this improved reagent. Figure 30 presents the results for the new transfected mESCs, and better rates for transfected/non-transfected colonies greatly improved. A parallel, control experiment was performed in order to, as before, determine if there is a toxic effect of Lipofectamine® 3000 on mESC. Like before, no visible effects were seen, yielding results very much alike those of Figure 28.

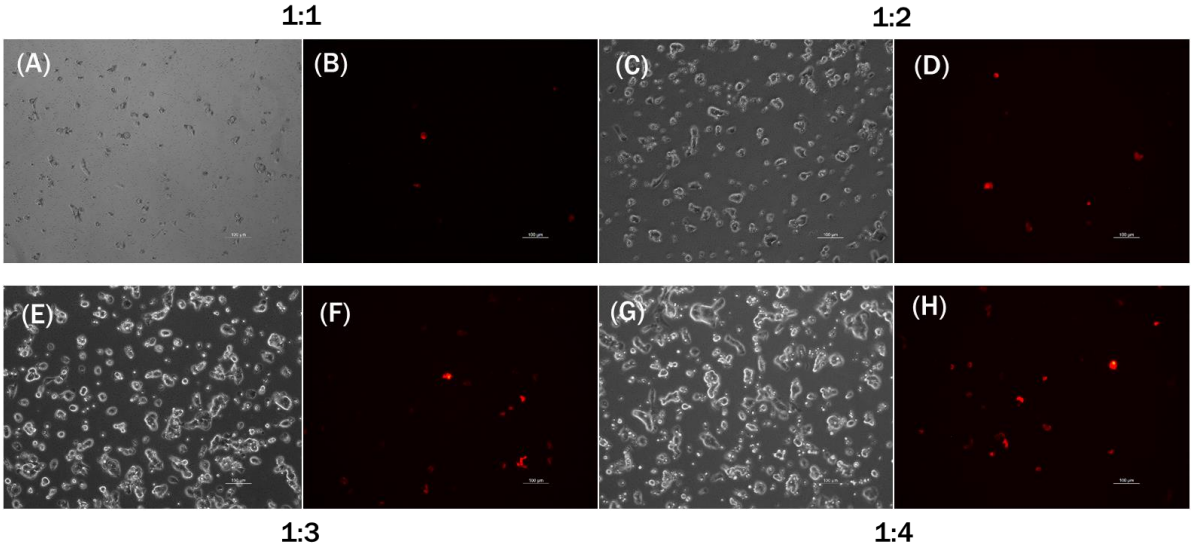

Figure 30 – Representative images of E14 mESC transfected with different Lipofectamine®3000:DNA ratios, with the DNA:Lipofectamine 3000 ratios adjacent. A, C, E and G represent phase contrast images, while B, D, F and H represent fluorescence images. Scale bar is 100µm.

Following transfection, transfected cells were meant to be selected through addition of puromycin, which would kill all unstransfected cells, while leaving plasmid-positive cells

unaffected. So, 48 hours after transfecting, puromycin was added with every medium exchange, as per determined in section 4.3.1. Nevertheless, using a concentration of 1µg/mL, which was the minimum concentration that would kill non-transfected cells, would result in the death of all cells in culture, either plasmid-positive or negative. As no cells survived this process, no further experiments were possible. After a new transfection, we applied a concentration of 0.5µg/mL puromycin, instead of 1µg/mL. This would provide a milder selection and allow us to obtain, in the very least, an enriched population of positively transfected cells. Alas, this smaller concentration would reveal itself to have the same effects as the preceding one. Again, there are no results to support this. This effect may be explained by the relatively low rate of transfection for these cells: as some colonies are only partly transfected (an example of a partially transfected mESC colony with an GFP-tagged protein can be seen in Figure 31, courtesy of a fellow lab colleague), killing the non-resistant cells may compromise the entire colonial structure, leading to further loss of both transfected and non-transfected cells. Another cause that may be contributing to the lack of general survivability may be the apoptotic cytokines and factors released by cells dying due to puromycin.

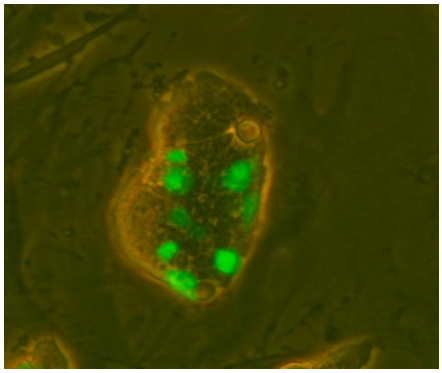

Figure 31 - Partly transfected mESC colony. This transfection was achieved by using the protocol described above, albeit with a GFP reporter-expressing plasmid. This image was kindly provived by a lab colleague.

As we weren't able to generate an enriched, much less pure, culture of transfected E14 mESC, three courses of action were considered: transfect these cells recurring to a different transfection method, as viral vectors or osmotic shock; or experiment with the same reagents (the same DNA samples and Lipofectamine® reagents) in another cell line. As it is reported to be easy to transfect (Tekle et al., 1991), are not as expensive to culture as mESC, and possess an active mitochondrial metabolism, the NIH-3T3 cell line was chosen for the next segment of the study.

4.4 SIRT3 SILENCING IN A DIFFERENTIATED CELL LINE: 3T3

As mESCs proved difficult to both efficiently transfect and select, we chose another cell line to proceed with the transfection protocol. This cell line would validate not only the

transfection protocol, but also the plasmid construct itself. If the transfection protocol would not work in these (documented to be easy to transfect) cells, this would point out that the transfection protocol was inadequate. If we manage to transfect these cells and observe a diminished levels of SIRT3, we must procure another transfection protocol, as the plasmid itself performs its inherent function.

4.4.1 3T3 cell line culturing

NIH-3T3 cells (hereby designated by 3T3 cells) are a cell line of mouse embryonic fibroblasts, firstly isolated in 1962 from National Institute of Health (NIH) Swiss mouse embryos. These cells, which are inhibited by benzodiazepines as well as contact, got their designation according to the "**3** day **t**ransfer, inoculum **3**x10^5 cells" method of passaging, and are nowadays a standardized and widely used fibroblast cell line.

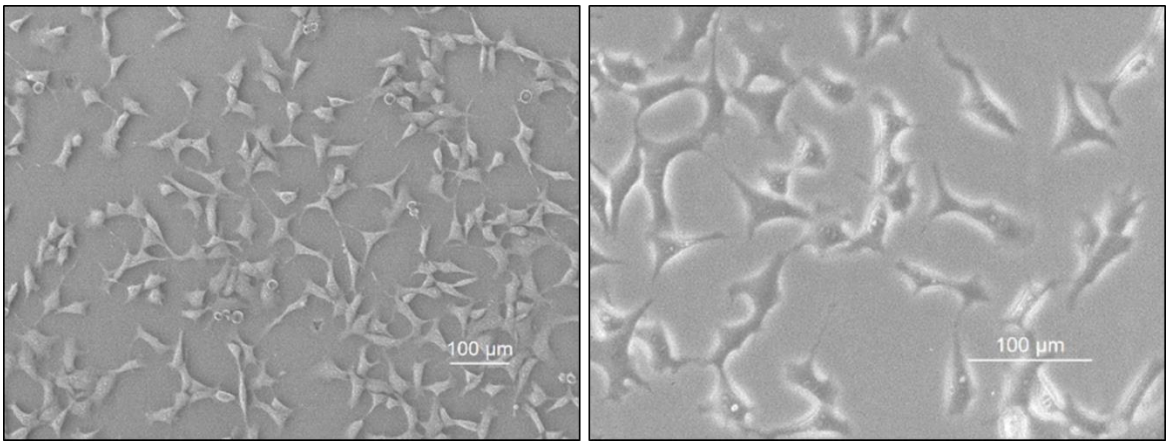

Figure 32 - The 3T3 cell line in culture with 60% confluence. Scale bar is 100µm.

Figure 32 shows 3T3 cells in culture, nearing adequate density of passaging. When compared with ESC, 3T3 cells are also cultured while adherent, but are much easier to culture: while they are contact-inhibited, their growth is fairly easy to follow, and the cell density does not hinder their growth nor survival. Therefore, they can be plated with much less accuracy than their pluripotent counterparts. Also, they grow in a basic, much cheaper culture medium, which does not need to be exchanged daily. Moreover, the detaching reagent used for these cells (TrypLE, an animal origin-free replacement for trypsin enzyme) is also less expensive than the Accutase used for mESC while maintaining a low toxicity and high efficiency. 3T3 cells suffer less from external factors as temperature or medium acidity. Finally, as 3T3 grow in a single-cell fashion (unlike E14 cells, which grow in colony structures), they should be easier to both transfect and select.

4.4.2 Selection conditions (SRB)

Similar to E14 cells, 3T3 cells were tested for the concentration of puromycin would kill all non-transfected cells and then will allow the selection of resistant cells. In a protocol very similar to that which was applied before, 3T3 cells were plated with a density of 5000 cells/cm^2, and exposed to different concentrations of the antibiotic. After 7 days after plating and 6 days of puromycin selection, the cells were fixed with PFA 4% and subjected to the SRB assay. The result for this assay are in Figure 33, which shows that concentrations of puromycin starting at 1.5µg/mL were able to virtually kill all non-resistant cells.

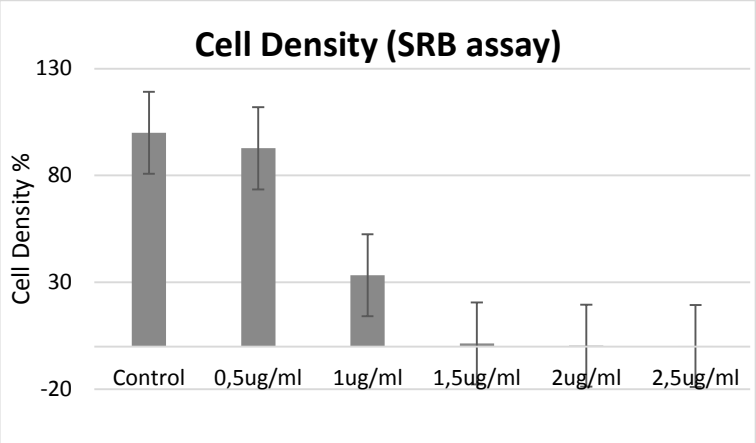

Figure 33 - Selection conditions for 3T3 cells. Cells were subject to sulforhodamine B colorimetric assay. Cells were fixed after 7 days in culture. These results were obtained from three independent experiments.

While selecting transfected cells, however, this concentration proved insufficient to kill all non-transfected cells in culture, forcing us to increase the amount of puromycin added to 2 µg/mL. This was probably due to the sheer number of plasmid-positive cells in the culture. As the puromycin resistance gene expressed by the plasmid encodes for Puromycin N-acetyltransferase, which inactivates puromycin by acetylation (Gómez Lahoz et al., 1991), puromycin degradation by these resistant cells does occur, thus lowering the effective puromycin concentration in the culture medium, to levels in which the available antibiotic is not enough to eliminate plasmid-negative cells.

4.4.3 Transfection & selection efficiency

As stated before, 3T3 cells were transfected following the same protocol as with E14 cells. Cells were transfected with a 1:1:1:1 mixture of all 4 shRNA-expressing plasmids. The first transfection, like before, was meant to assay the most effective ratio of DNA:Lipofectamine. Surprisingly, the most effective ratio of DNA:Lipofectamine was of 1:1, and so, this ratio was chosen for subsequent transfections. Transfections with 3T3 cells were

performed with Lipofectamine 2000, as it is considerately cheaper than Lipofectamine 3000, and we verified this reagent to be good enough in the 3T3 cells.

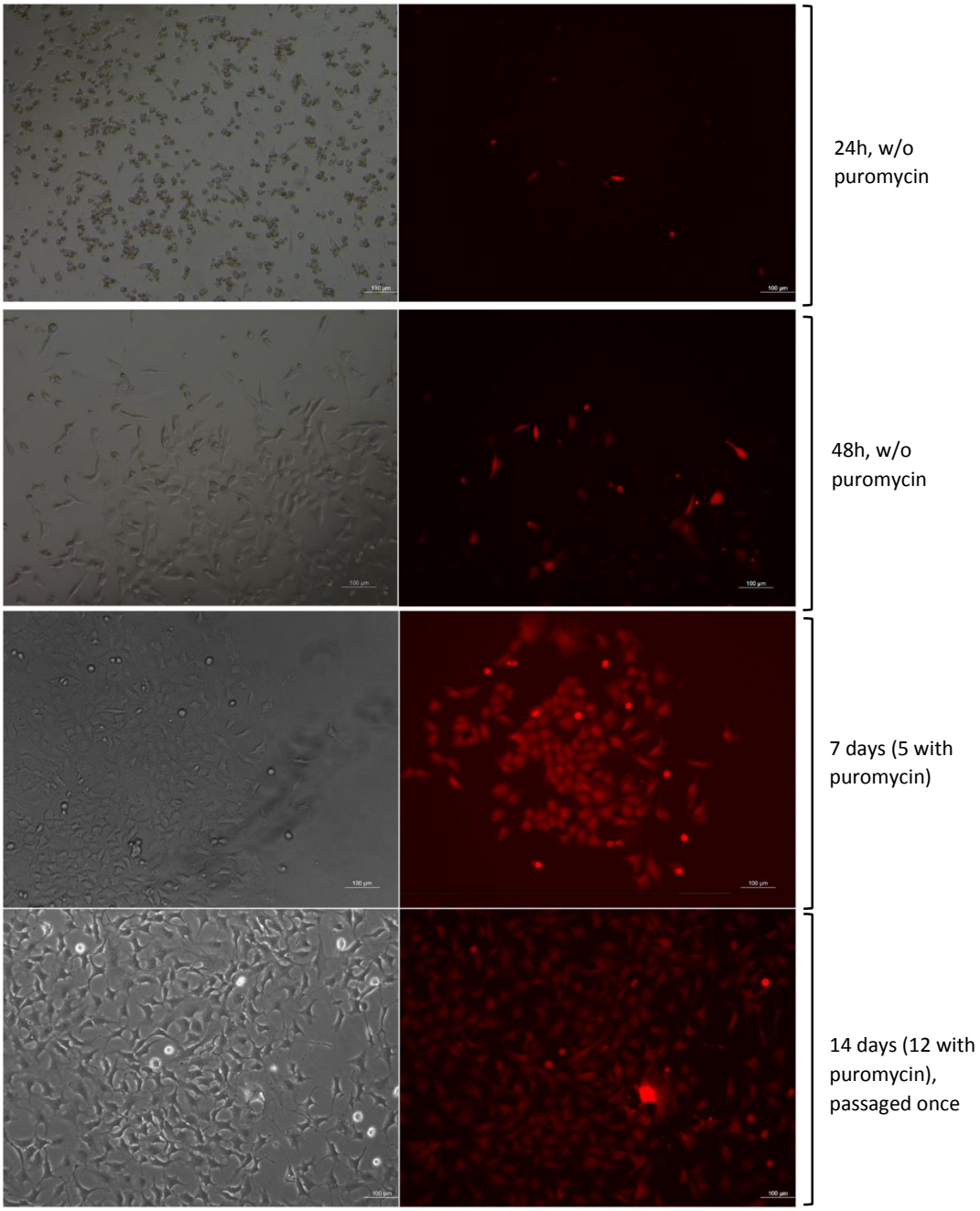

Figure 34 – Representative microphotographs of 3T3 cells, 24h after transfection, 48h after transfection. 3T3 cells, 7 days after transfecting, and 6 days after starting puromycin (2µg/ml) selection. Transfected 3T3 cell culture, 14 days after transfection, cultured in 2µg/ml puromycin. Scale bar is 100 µm.

Figure 34 shows the result of this transfection protocol in 3T3 cells, and subsequent selection, up to the point of obtaining a visually "pure" culture of fluorescent, puromycin resistant 3T3 cells. These cells able to be were cultured for a period of two months, circling 15 passages. During this period, both RNA and total protein content were collected to evaluate the silencing by SIRT3 shRNA expressed by the plasmids. In order to assure a transfected stock of 3T3 cells, cultures were also frozen and stored at -80°C. Furthermore, and in spite of not

knowing if in fact the levels of SIRT3 were knocked down, positive plasmid cells were dubbed “Knockdown”, of KD, for short.

4.4.4 Cytometry analysis of Transfected/Non-Transfected cells

In order to further characterize the transfection efficiency in 3T3 cells, we performed a flow cytometry analysis to measure the percentage of cells with red fluorescence, which would be exclusive to cells expressing the mCherry fluorescent reporter protein, encoded by our plasmid.

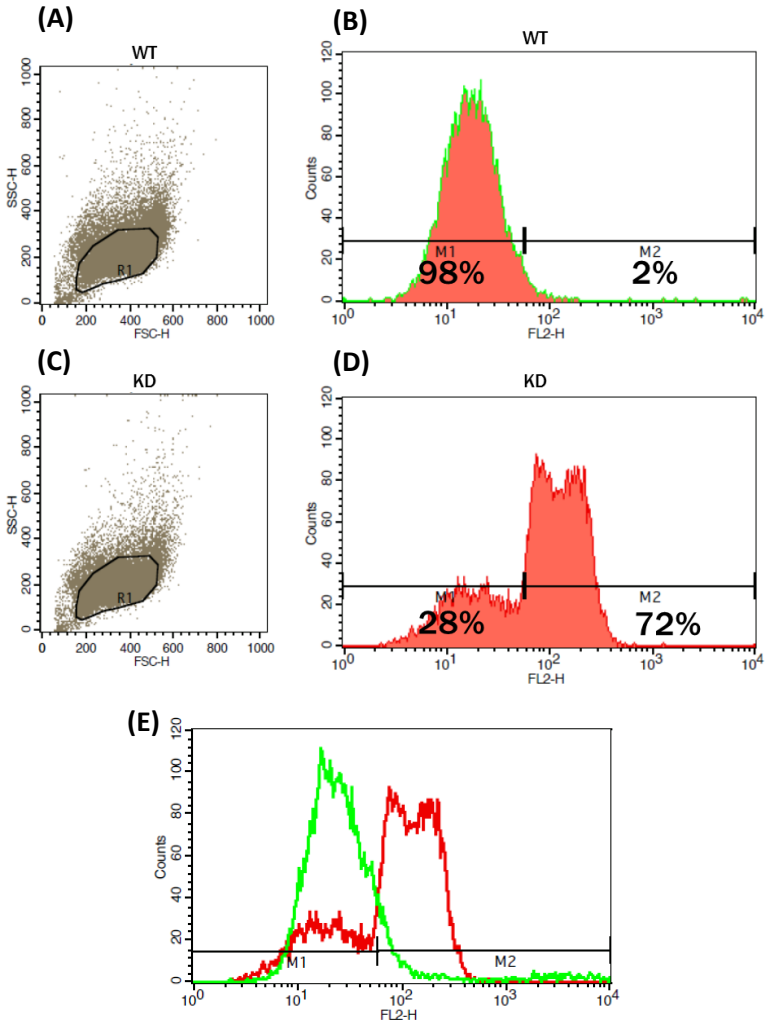

Figure 35 – Flow-cytometry results for the analysis of both transfected and non-transfected 3T3 cells. A and B refer to WT 3T3 cells. C and D refer to KD 3T3 cells. E shows the merge for both FL2 fluorescence analysis.

Figure 35 shows the flow-cytometry profiles for both transfected and non-transfected cells. After selecting the adequate gates for each cell sample (A and C), the percentage of red fluorescent cells was measured. While WT 3T3 cells show autofluorescence, as seen in Figure 35B, this fluorescence is lower than that of plasmid-positive cells (Figure 35D) and proper compensation was done when settings were defined during data acquisition. In spite of the entirety of transfected and selected 3T3 cells being visibly fluorescent (by fluorescence

microscopy), only approximately 70% of the KD 3T3 cells were fluorescent. As these cells were being cultured in selected conditions, we assume that this lack of fluorescence can be caused by photobleaching of mCherry, once the detaching of these cells was not conducted in the dark. Therefore, and although it couldn't be quantified, some of the low-fluorescing cells (as seen in Figure 35D) could be plasmid-positive cells, and not just autofluorescent cells. Nevertheless, these results show that both the transfection and selection of 3T3 cells was successful, and mean that we can now focus on evaluating the effectiveness of protein knockdown.

4.4.5 Evaluating SIRT3 silencing

Because transfection of 3T3 cells with the shRNA-expressing plasmid doesn't necessarily mean that the target protein is being silenced, we must evaluate the knockdown of SIRT3 levels, firstly through qRT-PCR (which is the quantification of expressed Sirt3 mRNA), and then by Immunocytochemistry and Western Blot (the protein).

4.4.5.1 qRT-PCR analysis

As explained before, shRNA-mediated silencing is done at the mRNA level. Therefore, it seemed logic to evaluate the silencing extension by qRT-PCR, the measurement of the levels of Sirt3 mRNA. The result for this evaluation (with a single experiment) is shown in Figure 36, and interestingly contrasts with the expected knockdown of Sirt3 mRNA, as there appears to be a slightly increased expression of these mRNA in transfected cells (KD) when compared with non-transfected cells (WT). The levels of the other two mitochondrial Sirtuins (Sirt4 and 5), as well as of Sirtuin1 (the major cellular deacetylase) were also evaluated to verify a possible unspecific silencing or a possible compensatory effect for Sirt3 silencing, but no effect could be visible to in Sirt1, 4 and 5 mRNA levels, similarly to Sirt3. As these results correspond to only one sample, a new qRT-PCR should be performed, with new RNA samples.

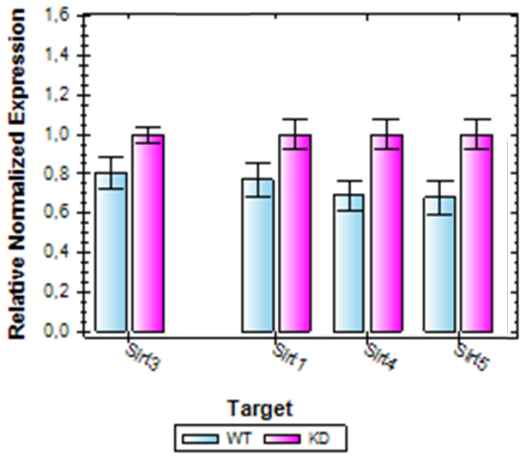

Figure 36 - qRT-PCR analysis for expression of mitochondrial Sirtuins (Sirt3, Sirt4, Sirt5) and also Sirt1 mRNA for both non-transfected (WT) and transfected (KD) cells. This image is the result of one experiment with 2 replicas for the same sample.

In spite of this unexpected result, there was a plausible and logical explanation for an increased expression of mRNA for Sirt3 in theoretically silenced cells. With siRNA mediated silencing, the mRNA for the target protein is either signaled to degradation by processed siRNA binding or, in an alternative manner, the siRNA binds to the target mRNA and blocks its translation in the ribosome. In this case, we hypothesize that Sirt3 mRNA is not being primarily targeted for degradation, but can be instead being repressed and hindered from being translated, and thus accumulating in the cells(Fellmann and Lowe, 2014; Rao et al., 2009). Besides, this repression of translation could be in fact lowering the levels of SIRT3 (protein), and the cell could try and compensate this by expressing more and more Sirt3 mRNA. All these factors would end up increasing the total levels of mRNA as measured by qRT-PCR. Therefore, the knockdown of SIRT3 must be confirmed through other techniques, specifically, downstream of mRNA, which is, the protein level.

4.4.5.2 Immunocytochemistry

The first manner by which the protein levels of SIRT3 was assayed was through Immunocytochemistry. Both transfected and non-transfected cells were plated in plastic cover-slips in which ICC would be performed. When the cells reached 70% confluence, they were fixed with a 4% PFA solution, blocked and incubated with an anti-SIRT3 primary antibody and correspondent secondary antibody. Cells were also stained with Hoecsht 33342 (DNA-binding dye) for co-localization purposes. This can be seen in Figure 37. mCherry fluorescence can be faintly perceived in transfected cells, and its weak fluorescence is most likely derived from the fixation process and the time that separates the moment of fixation from the time in which this ICC was performed. Nonetheless, said fluorescence could not be seen in non-transfected (WT) cells, as was expected. This proves that 3T3 cells do not possess auto fluorescence for this wavelength.

The resulting images for ICC failed to show a clear, definitive and obvious decrease in SIRT3. We were led to believe that either the silencing of SIRT3 was at least minimum, or entirely absent. Nevertheless, while it is possible to quantify protein expression by ICC, this measure is not precise, and would be more qualitative than quantitative. So, we took the total protein contents isolated from transfected 3T3 cultures and performed Western Blotting for SIRT3.

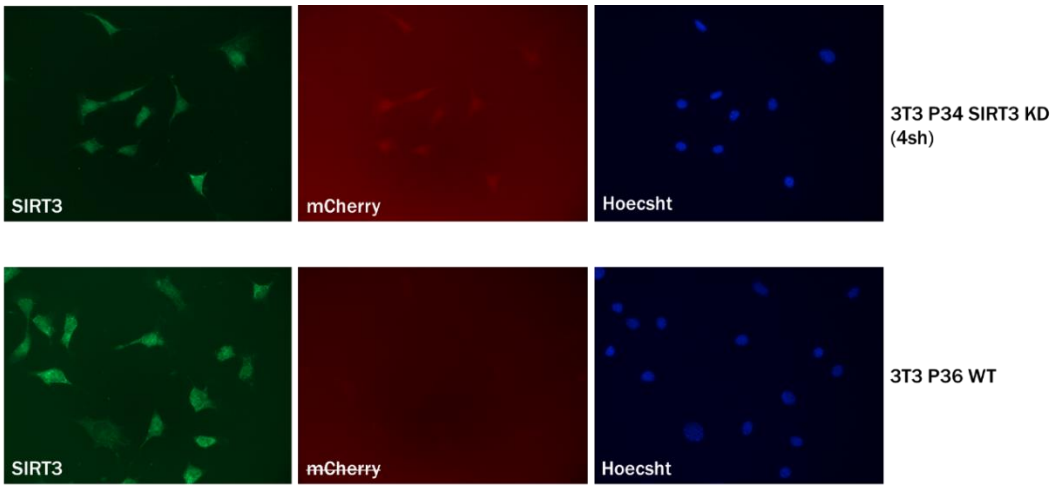

Figure 37 - Microphotographs of Immunostained 3T3 cultures. SIRT3 expression was evaluated, as well as the presence and absence of plasmid-derived mCherry. The first row shows transfected 3T3 cells, while the lower row shows non-transfected cells.

4.4.5.3 Western Blot analysis

Western Blotting provides the means to detect and quantify specific proteins with the use of an antibody, specific for a target protein. We performed western blotting for whole-cell protein samples from both WT and KD 3T3 cells.

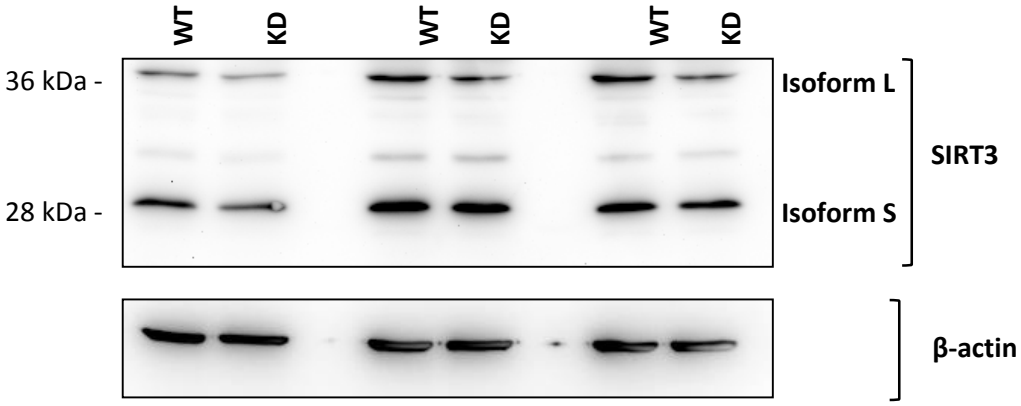

Figure 38 - Western blotting for transfected (KD) and non-transfected (WT) 3T3 cells.

In Figure 38, the various isoforms described for SIRT3 are evident. Considering, as mentioned above, that isoforms L (36kDa) and S (28kDa) as the two primary isoforms for SIRT3. Again, as expected after ICC, the differences between the levels of SIRT3 of non-transfected (WT) and transfected (KD) 3T3 cells are not visually evident, for neither isoform. Quantification was then performed, and the resulting image is shown in Figure 39.

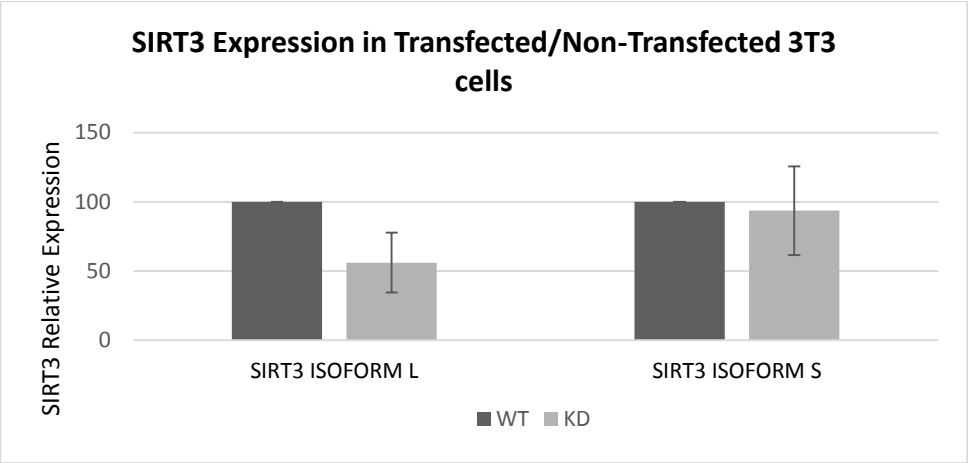

Figure 39 - Quantification for the expression of SIRT3's two canonical isoforms. This quantification is the result of a total of 6 individual protein samples.

As shown in section 4.2.1, the mRNA sequences targeted by all four shRNAs are common to both canonical isoforms of SIRT3. Therefore, we expected a similar silencing of both mitochondrial (isoform L) and cytoplasmic (isoform S) SIRT3, an observation that did not occur as per Figure 39: only the Isoform L appears to have its expression levels diminished. This led us to theorize that while both the fluorescence and puromycin resistance is conferred to 3T3 cells by all four plasmids, the knockdown capability of each shRNA sequence could differ from one another. The most logical step to take, from that moment on, was to transfect 3T3 cells with each individual plasmid, and yet again, verify the existence of SIRT3 knockdown.

4.4.6 Individual shRNA transfection

As stated, there could be a competitive effect between the four shRNA-expressing plasmids (once all them have the same promoter sequences and require the same machinery to be transcribed), with a specific mRNA-recognizing sequence being favored over the others. If a shRNA sequence with low knockdown capacity was being favored, this could explain the absence of obvious SIRT3 silencing. Therefore, each plasmid was individually transfected through the same protocol as before. Transfected cells were selected and cultured, also as described, and total protein contents were collected in order to perform Western Blot analysis.

4.4.6.1 Western Blot analysis

As before, Western Blot analysis for the protein contents of both transfected and non-transfected 3T3 cells was conducted. What was thought to be a turning point was yet again the inception for an inconclusive result. Again, antibody binding proved unreliable (Figure 40).

Labelling for the cytoplasmic isoform (28kDa, isoform S) largely surpassed the labelling on the longer isoform (36kDa, isoform L), and quantification suffered from this labeling.

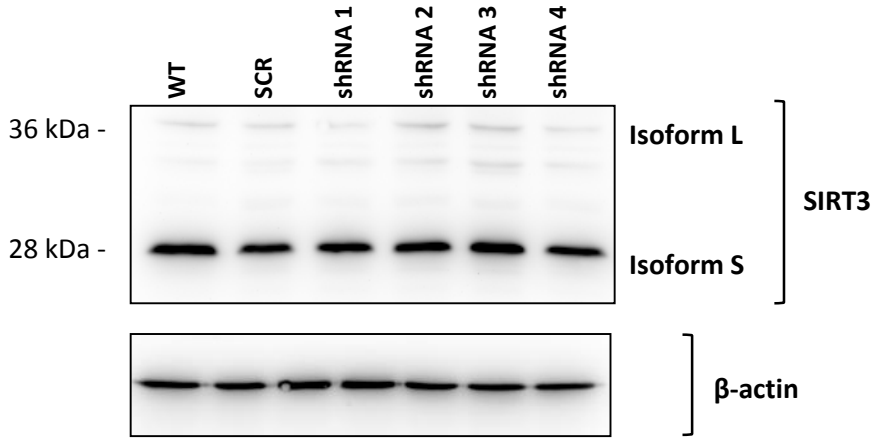

Figure 40 - Western blot for SIRT3 expression in non-transfected (WT), transfected with a scrambled shRNA (scr), and the individual SIRT3 shRNAs, 3T3 cells.

In Figure 41 lies the resulting quantification. In spite of what we postulated about the competition of each shRNA expression, the expression of one shRNA at a time doesn't seem to increase the knockdown efficiency. Strangely, the "silencing" pattern changed: it would appear that now, SIRT3 isoform S has a lesser expression when compared with its sibling isoform. Nonetheless, as this analysis is the result of one set of protein samples, the assay should be repeated and statistically analyzed.

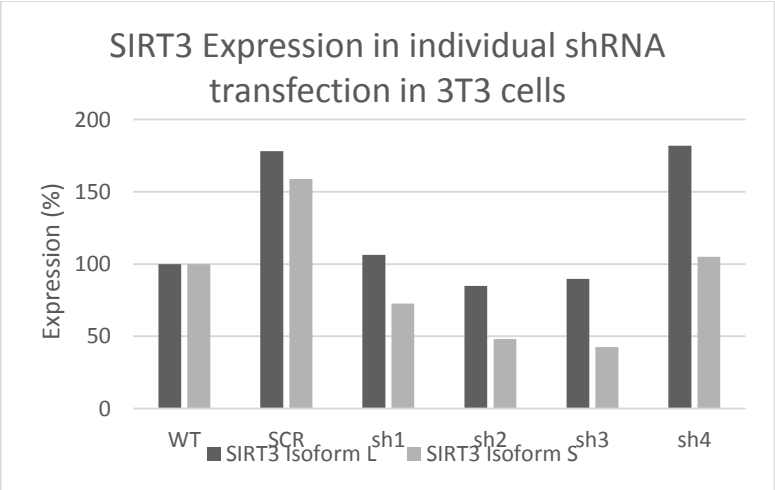

Figure 41 - Quantification for the expression of SIRT3's two canonical isoforms. This quantification is the result of a total of one individual set of protein samples.

Because this experiment also failed to clearly knockdown SIRT3's expression (of either isoform), we couldn't prove if a) some of the shRNA-expressing plasmids present a stronger knockdown capability (although shRNA4 could be thought as unable to knockdown SIRT3, when comparing with the other shRNA sequences), and b) using all four shRNAs at the same

time presents a more pronounced knockdown of SIRT3's levels. Again, more assays should be performed, and perhaps, validated with a different anti-SIRT3 antibody (because, as visible throughout this essay, SIRT3 immunostaining presented different labeling, even when using the same samples).

After these negative results, we searched for what could be negatively affecting our silencing, because, as has been shown, the cells are definitely transfected. Many causes could potentially explain why the silencing appears non-existent. We looked for clues to what mechanisms could inhibit this silencing (as the shRNA was, most likely, and alike mCherry and PAC, being expressed). It has been reported that the expression of SIRT3 vary, depending on the proliferative state of cells (Abdel Khalek et al., 2014). Khalek and collaborators found that during the proliferative state of mouse myoblasts (C2C12), the expression of SIRT3 is negligible, and greatly increased when cells stopped proliferating and started to differentiate. Unfortunately, this work does not specify the silenced isoform(s) of SIRT3. Nevertheless, a parallelism could be drawn to our work: the assayed protein samples for transfected and non-transfected 3T3 were all collected nearing confluence. If the SIRT3 expression pattern in 3T3 cells mimics that of C2C12 cells, one could argue that SIRT3 expression would be also greatly increased, and the short-hairpin silencing mechanisms could not mitigate this increase of their target sequence. Therefore, in the future, these assays should be repeated bearing this work in mind. Also, the selected sequences may not be the right/adequate sequences to block translation/degrade SIRT3 mRNA. Furthermore, plasmids should be sequenced to confirm the sequences provided by the manufacturer, as the slightest mis-match of the shRNA sequence can void its silencing capability (Taxman et al., 2006).

5 CONCLUSION AND FINAL REMARKS

This work was meant to be a stepping stone to the establishment of a silencing protocol, aiming to provide means to protein silencing in mouse Embryonic Stem Cells, by specifically targeting a mitochondrial protein, SIRT3, a metabolically relevant protein with the ability to, overall, regulate the mitochondrial metabolism. Besides a possible evaluation of the mechanisms and relevance of SIRT3 in the pluripotency and differentiation of mESC, this work would provide a tool to silence any given protein in our working models, as long as its coding sequence was known. It can be said that the basis for this tool are set.

Transfection couldn't be performed on E14 ES cells, but it seemed relatively stable in 3T3 cells. The transfection and selection of 3T3 cells was accomplished: cells were both resistant to antibiotic and fluorescent; both attributes are conferred by the transfected plasmid. If mESC transfection is to be achieved, a possible solution to surpass the inability to obtain an enriched, transfected mESC culture would be by turning to viral vectors. Increasing the starting number of plasmid positive cells would indubitably ease the selection process, yielding sturdier colonies, and generating steadier cultures.

In spite of the success in transfecting 3T3 cells with our shRNA-expressing plasmids, the silencing rates are, at the very least, dubious. The results in 3T3 cells, when transfecting either all four shRNA-expressing plasmids, or each plasmid individually, the silencing rate hardly reached 50%, was regarded as an underachievement, compared to the promising and reported capabilities of this silencing technique. The next steps should include the return to the laboratory, and re-evaluate the silencing rate in 3T3 cells in a non-confluent state. If this does not prove to surpass the low silencing rate, we must look into de shRNA sequences. As discussed before, the shRNA sequences may not be the most adequate for our sequence, and so, the next step would be that of the choice of different shRNA sequences for SIRT3.

Closing this work, I'd like to state that this work, the establishment of the said protocol, while not as successful as initially predicted, should not be entirely abandoned. This work served, at least to show the hurdles of both transfection, and protein silencing. Seeing as numerous reports of transfection (and protein silencing) are achieved in mESC, in general, and E14Tg2.a in particular, and Armed with this knowledge, we may yet succeed, if only should we press on.

6 REFERENCES

Abdel Khalek, W., Cortade, F., Ollendorff, V., Lapasset, L., Tintignac, L., Chabi, B., and Wrutniak-Cabello, C. (2014). SIRT3, a Mitochondrial NAD+-Dependent Deacetylase, Is Involved in the Regulation of Myoblast Differentiation. PLoS One *9*, e114388.

Abe, K., Niwa, H., Iwase, K., Takiguchi, M., Mori, M., Abé, S.-I., Abe, K., and Yamamura, K.-I. (1996). Endoderm-Specific Gene Expression in Embryonic Stem Cells Differentiated to Embryoid Bodies. Exp. Cell Res. *229*, 27–34.

Altman, J., and Das, G.D. (1967). Postnatal Neurogenesis in the Guinea-pig. Nature *214*, 1098–1101.

Ameres, S.L., Martinez, J., and Schroeder, R. (2007). Molecular basis for target RNA recognition and cleavage by human RISC. Cell *130*, 101–112.

Aubert, J., Dunstan, H., Chambers, I., and Smith, A. (2002). Functional gene screening in embryonic stem cells implicates Wnt antagonism in neural differentiation. Nat. Biotechnol. *20*, 1240–1245.

Baharvand, H., and Matthaei, K.I. (2003). The ultrastructure of mouse embryonic stem cells. Reprod. Biomed. Online *7*, 330–335.

Bannai, S. (1992). Use of 2-mercaptoethanol in cell culture. Hum. Cell Off. J. Hum. Cell Res. Soc. *5*, 292–297.

Bao, J., Lu, Z., Joseph, J.J., Carabenciov, D., Dimond, C.C., Pang, L., Samsel, L., McCoy, J.P., Leclerc, J., Nguyen, P., et al. (2010). Characterization of the murine SIRT3 mitochondrial localization sequence and comparison of mitochondrial enrichment and deacetylase activity of long and short SIRT3 isoforms. J. Cell. Biochem. *110*, n/a – n/a.

Barberi, T., Klivenyi, P., Calingasan, N.Y., Lee, H., Kawamata, H., Loonam, K., Perrier, A.L., Bruses, J., Rubio, M.E., Topf, N., et al. (2003). Neural subtype specification of fertilization and nuclear transfer embryonic stem cells and application in parkinsonian mice. Nat. Biotechnol. *21*, 1200–1207.

Bianco, P., Riminucci, M., Gronthos, S., and Robey, P. (2001). Bone marrow stromal stem cells: nature, biology, and potential applications. Stem Cells 180–192.

Brown, K., Xie, S., Qiu, X., Mohrin, M., Shin, J., Liu, Y., Zhang, D., Scadden, D.T., and Chen, D. (2013). SIRT3 reverses aging-associated degeneration. Cell Rep. *3*, 319–327.

Brunet, A. (2004). Stress-Dependent Regulation of FOXO Transcription Factors by the SIRT1 Deacetylase. Science (80-.). *303*, 2011–2015.

Cahan, P., and Daley, G.Q. (2013). Origins and implications of pluripotent stem cell variability and heterogeneity. Nat. Rev. Mol. Cell Biol. *14*, 357–368.

Calvanese, V., Lara, E., Suarez-Alvarez, B., Abu Dawud, R., Vazquez-Chantada, M., Martinez-Chantar, M.L., Embade, N., Lopez-Nieva, P., Horrillo, A., Hmadcha, A., et al. (2010). Sirtuin 1 regulation of developmental genes during differentiation of stem cells. Proc. Natl. Acad. Sci. *107*, 13736–13741.

Chambers, I., Colby, D., Robertson, M., Nichols, J., Lee, S., Tweedie, S., and Smith, A. (2003). Functional expression cloning of Nanog, a pluripotency sustaining factor in embryonic stem cells. Cell *113*, 643–655.

Chen, C.-T., Hsu, S.-H., and Wei, Y.-H. (2012). Mitochondrial bioenergetic function and metabolic plasticity in stem cell differentiation and cellular reprogramming. Biochim. Biophys. Acta *1820*, 571–576.

Cheng, H.-L., Mostoslavsky, R., Saito, S., Manis, J.P., Gu, Y., Patel, P., Bronson, R., Appella, E., Alt, F.W., and Chua, K.F. (2003). Developmental defects and p53 hyperacetylation in Sir2 homolog (SIRT1)-deficient mice. Proc. Natl. Acad. Sci. U. S. A. *100*, 10794–10799.

Cheng, J., Dutra, A., Takesono, A., Garrett-Beal, L., and Schwartzberg, P.L. (2004). Improved generation of C57BL/6J mouse embryonic stem cells in a defined serum-free media. Genesis *39*, 100–104.

Cho, Y.M., Kwon, S., Pak, Y.K., Seol, H.W., Choi, Y.M., Park, D.J., Park, K.S., and Lee, H.K. (2006). Dynamic changes in mitochondrial biogenesis and antioxidant enzymes during the spontaneous differentiation of human embryonic stem cells. Biochem. Biophys. Res. Commun. *348*, 1472–1478.

Christophorou, M. a, Castelo-Branco, G., Halley-Stott, R.P., Oliveira, C.S., Loos, R., Radzisheuskaya, A., Mowen, K. a, Bertone, P., Silva, J.C.R., Zernicka-Goetz, M., et al. (2014). Citrullination regulates pluripotency and histone H1 binding to chromatin. Nature *507*, 104–108.

Chung, S., and Dzeja, P. (2007). Mitochondrial oxidative metabolism is required for the cardiac differentiation of stem cells. Nat. Clin. Pract. … *4*, 1–12.

Conti, L., Pollard, S.M., Gorba, T., Reitano, E., Toselli, M., Biella, G., Sun, Y., Sanzone, S., Ying, Q.-L., Cattaneo, E., et al. (2005). Niche-independent symmetrical self-renewal of a mammalian tissue stem cell. PLoS Biol. *3*, e283.

Cooper, H.M., Huang, J.-Y., Verdin, E., and Spelbrink, J.N. (2009). A new splice variant of the mouse SIRT3 gene encodes the mitochondrial precursor protein. PLoS One *4*, e4986.

Evans, M.J., and Kaufman, M.H. (1981). Establishment in culture of pluripotential cells from mouse embryos. Nature *292*, 154–156.

Facucho-Oliveira, J.M., and St John, J.C. (2009). The relationship between pluripotency and mitochondrial DNA proliferation during early embryo development and embryonic stem cell differentiation. Stem Cell Rev. *5*, 140–158.

Facucho-Oliveira, J.M., Alderson, J., Spikings, E.C., Egginton, S., and St John, J.C. (2007). Mitochondrial DNA replication during differentiation of murine embryonic stem cells. J. Cell Sci. *120*, 4025–4034.

Fellmann, C., and Lowe, S.W. (2014). Stable RNA interference rules for silencing. Nat. Cell Biol. *16*, 10–18.

Finkel, T., Deng, C.-X., and Mostoslavsky, R. (2009). Recent progress in the biology and physiology of sirtuins. Nature *460*, 587–591.

Folmes, C., Nelson, T., and Terzic, A. (2011a). Energy metabolism in nuclear reprogramming. Biomark. Med. *5*, 715–729.

Folmes, C., Dzeja, P., Nelson, T., and Terzic, A. (2012). Metabolic plasticity in stem cell homeostasis and differentiation. Cell Stem Cell *11*, 596–606.

Folmes, C.D.L., Nelson, T.J., Martinez-Fernandez, A., Arrell, D.K., Lindor, J.Z., Dzeja, P.P., Ikeda, Y., Perez-Terzic, C., and Terzic, A. (2011b). Somatic oxidative bioenergetics transitions into pluripotency-dependent glycolysis to facilitate nuclear reprogramming. Cell Metab. *14*, 264–271.

Giralt, A., Hondares, E., Villena, J.A., Ribas, F., Díaz-Delfín, J., Giralt, M., Iglesias, R., and Villarroya, F. (2011). Peroxisome proliferator-activated receptor-gamma coactivator-1alpha controls transcription of the Sirt3 gene, an essential component of the thermogenic brown adipocyte phenotype. J. Biol. Chem. *286*, 16958–16966.

Gómez Lahoz, E., López de Haro, M.S., Nieto, a, and Esponda, P. (1991). Use of puromycin N-acetyltransferase (PAC) as a new reporter gene in transgenic animals. Nucleic Acids Res. *19*, 3465.

Gonzales, K.A.U., and Ng, H.-H. (2011). FoxO: A New Addition to the ESC Cartel. Cell Stem Cell *9*, 181–183.

Grayson, W., and Zhao, F. (2006). Effects of hypoxia on human mesenchymal stem cell expansion and plasticity in 3D constructs. J. Cell. … *339*, 331–339.

Haeckel, E. (1879). Natürliche Schöpfungsgeschichte (Berlin: G. Reimer).

Haigis, M.C., and Guarente, L.P. (2006). Mammalian sirtuins - Emerging roles in physiology, aging, and calorie restriction. Genes Dev. *20*, 2913–2921.

Hanahan, D. (1983). Studies on transformation of Escherichia coli with plasmids. J. Mol. Biol. *166*, 557–580.

Hanna, J.H., Saha, K., and Jaenisch, R. (2010). Pluripotency and cellular reprogramming: Facts, hypotheses, unresolved issues. Cell *143*, 508–525.

Hu, B., Guo, Y., Chen, C., Li, Q., Niu, X., Guo, S., Zhang, A., Wang, Y., and Deng, Z. (2014). Repression of SIRT1 Promotes the Differentiation of Mouse Induced Pluripotent Stem Cells into Neural Stem Cells. Cell. Mol. Neurobiol. *34*, 905–912.

Imai, S., Armstrong, C.M., Kaeberlein, M., and Guarente, L. (2000). Transcriptional silencing and longevity protein Sir2 is an NAD-dependent histone deacetylase. Nature *403*, 795–800.

Invitrogen(tm) by life technologies (2000). Lipofectamine ® 2000 Reagent. 1–2.

Janjic, D., and Wollheim, C.B. (1992). Effect of 2-mercaptoethanol on glutathione levels, cystine uptake and insulin secretion in insulin-secreting cells. Eur. J. Biochem. *210*, 297–304.

Kawamura, Y., and Uchijima, Y. (2010). Sirt3 protects in vitro–fertilized mouse preimplantation embryos against oxidative stress–induced p53-mediated developmental arrest. J. … *120*.

Kim, J., Chu, J., Shen, X., Wang, J., and Orkin, S.H. (2008). An Extended Transcriptional Network for Pluripotency of Embryonic Stem Cells. Cell *132*, 1049–1061.

Klimo, P., Kestle, J.R.W., MacDonald, J.D., and Schmidt, R.H. (2004). Marked reduction of cerebral vasospasm with lumbar drainage of cerebrospinal fluid after subarachnoid hemorrhage. J. Neurosurg. *100*, 215–224.

Lambeth, L.S., and Smith, C.A. (2013). siRNA Design (Totowa, NJ: Humana Press).

Langley, E. (2002). Human SIR2 deacetylates p53 and antagonizes PML/p53-induced cellular senescence. EMBO J. *21*, 2383–2396.

Li, M., He, Y., Dubois, W., Wu, X., Shi, J., and Huang, J. (2012). Distinct Regulatory Mechanisms and Functions for p53-Activated and p53-Repressed DNA Damage Response Genes in Embryonic Stem Cells. Mol. Cell *46*, 30–42.

Lin, H.-T., Otsu, M., and Nakauchi, H. (2013). Stem cell therapy: an exercise in patience and prudence. Philos. Trans. R. Soc. Lond. B. Biol. Sci. *368*, 20110334.

Lombard, D.B., Alt, F.W., Cheng, H.-L., Bunkenborg, J., Streeper, R.S., Mostoslavsky, R., Kim, J., Yancopoulos, G., Valenzuela, D., Murphy, A., et al. (2007). Mammalian Sir2 homolog SIRT3 regulates global mitochondrial lysine acetylation. Mol. Cell. Biol. *27*, 8807–8814.

Martin, G.R. (1981). Isolation of a pluripotent cell line from early mouse embryos cultured in medium conditioned by teratocarcinoma stem cells. Proc. Natl. Acad. Sci. U. S. A. *78*, 7634–7638.

Mathieu, J., Zhou, W., Xing, Y., Sperber, H., Ferreccio, A., Agoston, Z., Kuppusamy, K.T., Moon, R.T., and Ruohola-Baker, H. (2014). Hypoxia-inducible factors have distinct and stage-specific roles during reprogramming of human cells to pluripotency. Cell Stem Cell *14*, 592–605.

Maurisse, R., De Semir, D., Emamekhoo, H., Bedayat, B., Abdolmohammadi, A., Parsi, H., and Gruenert, D.C. (2010). Comparative transfection of DNA into primary and transformed mammalian cells from different lineages. BMC Biotechnol. *10*, 9.

Maximow, A.A. (2009). The lymphocyte as a stem cell, common to different blood elements in embryonic development and during the post-fetal life of mammals: Lecture with a demonstration, held at a special meeting of the Berlin Hematological Society on 1 June 1909. Cell. Ther. Transplant. *1*, 14–24.

Niwa, H., Ogawa, K., Shimosato, D., and Adachi, K. (2009). A parallel circuit of LIF signalling pathways maintains pluripotency of mouse ES cells. Nature *460*, 118–122.

Nzytech (2013). NZY5a Competent Cells - Transformation Protocol.

Pattappa, G., Heywood, H.K., de Bruijn, J.D., and Lee, D. a (2011). The metabolism of human mesenchymal stem cells during proliferation and differentiation. J. Cell. Physiol. *226*, 2562–2570.

Peister, A., Mellad, J. a, Larson, B.L., Hall, B.M., Gibson, L.F., and Prockop, D.J. (2004). Adult stem cells from bone marrow (MSCs) isolated from different strains of inbred mice vary in surface epitopes, rates of proliferation, and differentiation potential. Blood *103*, 1662–1668.

Pereira, S.L., Grãos, M., Rodrigues, A.S., Anjo, S.I., Carvalho, R. a, Oliveira, P.J., Arenas, E., and Ramalho-Santos, J. (2013). Inhibition of Mitochondrial Complex III Blocks Neuronal Differentiation and Maintains Embryonic Stem Cell Pluripotency. PLoS One *8*, e82095.

Pereira, S.L., Rodrigues, A.S., Sousa, M.I., Correia, M., Perestrelo, T., and Ramalho-Santos, J. (2014). From gametogenesis and stem cells to cancer: Common metabolic themes. Hum. Reprod. Update *0*, 1–20.

Rafalski, V. a, Mancini, E., and Brunet, A. (2012). Energy metabolism and energy-sensing pathways in mammalian embryonic and adult stem cell fate. J. Cell Sci. *125*, 5597–5608.

Ramalho-Santos, M., and Willenbring, H. (2007). On the Origin of the Term “Stem Cell.” Cell Stem Cell *1*, 35–38.

Ramalho-Santos, J., Varum, S., Amaral, S., Mota, P.C., Sousa, A.P., and Amaral, A. (2009). Mitochondrial functionality in reproduction: from gonads and gametes to embryos and embryonic stem cells. Hum. Reprod. Update *15*, 553–572.

Rao, D.D., Vorhies, J.S., Senzer, N., and Nemunaitis, J. (2009). siRNA vs. shRNA: similarities and differences. Adv. Drug Deliv. Rev. *61*, 746–759.

Robinson, J.P., Narayanan, K., Ragheb, K., and Lawler, G. (1997). Defects in intracellular oxidative undergoing apoptosis metabolism of neutrophils. *61*, 481–488.

Rodrigues, A.S., Correia, M., Gomes, A., Pereira, S.L., Perestrelo, T., Sousa, M.I., and Ramalho-Santos, J. (2015). Dichloroacetate, the Pyruvate Dehydrogenase Complex and the Modulation of mESC Pluripotency. PLoS One *10*, e0131663.

Rodriguez, R.M., Fernandez, a F., and Fraga, M.F. (2013). Role of sirtuins in stem cell differentiation. Genes Cancer *4*, 105–111.

Saunders, L.R., Sharma, A.D., Tawney, J., Nakagawa, M., Okita, K., Yamanaka, S., Willenbring, H., and Verdin, E. (2010). miRNAs regulate SIRT1 expression during mouse embryonic stem cell differentiation and in adult mouse tissues. Aging (Albany. NY). *2*, 415–431.

Schieke, S.M., Ma, M., Cao, L., McCoy, J.P., Liu, C., Hensel, N.F., Barrett, A.J., Boehm, M., and Finkel, T. (2008). Mitochondrial Metabolism Modulates Differentiation and Teratoma Formation Capacity in Mouse Embryonic Stem Cells. J. Biol. Chem. *283*, 28506–28512.

Shi, T., Wang, F., Stieren, E., and Tong, Q. (2005). SIRT3, a mitochondrial sirtuin deacetylase, regulates mitochondrial function and thermogenesis in brown adipocytes. J. Biol. Chem. *280*, 13560–13567.

Signer, R.A.J., and Morrison, S.J. (2013). Mechanisms that Regulate Stem Cell Aging and Life Span. Cell Stem Cell *12*, 152–165.

Simsek, T., Kocabas, F., Zheng, J., Deberardinis, R.J., Mahmoud, A.I., Olson, E.N., Schneider, J.W., Zhang, C.C., and Sadek, H. a (2010). The distinct metabolic profile of hematopoietic stem cells reflects their location in a hypoxic niche. Cell Stem Cell *7*, 380–390.

Singh, U., Quintanilla, R.H., Grecian, S., Gee, K.R., Rao, M.S., and Lakshmipathy, U. (2012). Novel Live Alkaline Phosphatase Substrate for Identification of Pluripotent Stem Cells. Stem Cell Rev. Reports *8*, 1021–1029.

Skalli, O., Pelte, M.F., Peclet, M.C., Gabbiani, G., Gugliotta, P., Bussolati, G., Ravazzola, M., and Orci, L. (1989). Alpha-smooth muscle actin, a differentiation marker of smooth muscle cells, is present in microfilamentous bundles of pericytes. J. Histochem. Cytochem. *37*, 315–321.

Sousa, M.I., Rodrigues, A.S., Pereira, S., Perestrelo, T., Correia, M., and Ramalho-Santos, J. (2013). Mitochondrial mechanisms of metabolic reprogramming in proliferating cells. University of Coimbra.

Southwood, C.M., Peppi, M., Dryden, S., Tainsky, M. a., and Gow, A. (2007). Microtubule deacetylases, SirT2 and HDAC6, in the nervous system. Neurochem. Res. *32*, 187–195.

Stanley, I. a, Ribeiro, S.M., Giménez-Cassina, A., Norberg, E., and Danial, N.N. (2013). Changing appetites: the adaptive advantages of fuel choice. Trends Cell Biol. *24*.

Storm, M.P., Bone, H.K., Beck, C.G., Bourillot, P.Y., Schreiber, V., Damiano, T., Nelson, A., Savatier, P., and Welham, M.J. (2007). Regulation of nanog expression by phosphoinositide 3-kinase-dependent signaling in murine embryonic stem cells. J. Biol. Chem. *282*, 6265–6273.

Suda, T., Takubo, K., and Semenza, G.L. (2011). Metabolic regulation of hematopoietic stem cells in the hypoxic niche. Cell Stem Cell *9*, 298–310.

Taxman, D.J., Livingstone, L.R., Zhang, J., Conti, B.J., Iocca, H. a, Williams, K.L., Lich, J.D., Ting, J.P.-Y., and Reed, W. (2006). Criteria for effective design, construction, and gene knockdown by shRNA vectors. BMC Biotechnol. *6*, 7.

Tekle, E., Astumian, R.D., and Chock, P.B. (1991). Electroporation by using bipolar oscillating electric field: an improved method for DNA transfection of NIH 3T3 cells. Proc. Natl. Acad. Sci. U. S. A. *88*, 4230–4234.

Thermo Scientific, D. (2011). NanoDrop: Assessment of Nucleic Acid Purity. Protoc. Prod. Manuals 1–2.

Upadhyay, M., Samal, J., Kandpal, M., Singh, O.V., and Vivekanandan, P. (2013). The Warburg effect: insights from the past decade. Pharmacol. Ther. *137*, 318–330.

Vara, J., Malpartida, F., Hopwood, D. a., and Jimenez, a. (1985). Cloning and expression of a puromycin N-acetyl transferase gene from Streptomyces alboniger in Streptomyces lividans and Escherichia coli. Gene *33*, 197–206.

Varum, S., Momcilović, O., Castro, C., Ben-Yehudah, A., Ramalho-Santos, J., and Navara, C.S. (2009). Enhancement of human embryonic stem cell pluripotency through inhibition of the mitochondrial respiratory chain. Stem Cell Res. *3*, 142–156.

Varum, S., Rodrigues, A.S., Moura, M.B., Momcilovic, O., Easley IV, C.A., Ramalho-Santos, J., van Houten, B., and Schatten, G. (2011). Energy metabolism in human pluripotent stem cells and their differentiated counterparts. PLoS One *6*, e20914.

Wang, X.-Q., Shao, Y., Ma, C.-Y., Chen, W., Sun, L., Liu, W., Zhang, D.-Y., Fu, B.-C., Liu, K.-Y., Jia, Z.-B., et al. (2014). Decreased SIRT3 in aged human mesenchymal stromal/stem cells increases cellular susceptibility to oxidative stress. J. Cell. Mol. Med. *XX*, 1–13.

Wang, Z.-X., Teh, C.H.-L., Kueh, J.L.L., Lufkin, T., Robson, P., and Stanton, L.W. (2007). Oct4 and Sox2 directly regulate expression of another pluripotency transcription factor, Zfp206, in embryonic stem cells. J. Biol. Chem. *282*, 12822–12830.

Warburg, O. (1956). On the origin of cancer cells. Science (80-.). *123*, 309–314.

Ward, C.M., Barrow, K.M., and Stern, P.L. (2004). Significant variations in differentiation properties between independent mouse ES cell lines cultured under defined conditions. Exp. Cell Res. *293*, 229–238.

Weisbart, R., and Kwan, L. (1987). Human GM-CSF primes neutrophils for enhanced oxidative metabolism in response to the major physiological chemoattractants. … 18–21.

Wittmann, J. (2006). siRNA , shRNA , miRNA - different approaches for gene silencing.

Wray, J., Kalkan, T., Gomez-Lopez, S., Eckardt, D., Cook, A., Kemler, R., and Smith, A. (2011). Inhibition of glycogen synthase kinase-3 alleviates Tcf3 repression of the pluripotency network and increases embryonic stem cell resistance to differentiation. Nat. Cell Biol. *13*, 838–845.

Xu, J. (2011). Viral and Plasmid Transduction Systems : Methods to Modify Immune Cells for Cancer Immunotherapy.

Yanes, O., Clark, J., and Wong, D. (2010). Metabolic oxidation regulates embryonic stem cell differentiation. Nat. Chem. … *6*, 411–417.

Yang, Y., Hubbard, B.P., Sinclair, D.A., and Tong, Q. (2010). Characterization of murine SIRT3 transcript variants and corresponding protein products. J. Cell. Biochem. *111*, 1051–1058.

Ying, Q.-L., Wray, J., Nichols, J., Batlle-Morera, L., Doble, B., Woodgett, J., Cohen, P., and Smith, A. (2008). The ground state of embryonic stem cell self-renewal. Nature *453*, 519–523.

Yoshida, Y., Takahashi, K., Okita, K., Ichisaka, T., and Yamanaka, S. (2009). Hypoxia enhances the generation of induced pluripotent stem cells. Cell Stem Cell *5*, 237–241.

Zhang, J., Tam, W.-L., Tong, G.Q., Wu, Q., Chan, H.-Y., Soh, B.-S., Lou, Y., Yang, J., Ma, Y., Chai, L., et al. (2006). Sall4 modulates embryonic stem cell pluripotency and early embryonic development by the transcriptional regulation of Pou5f1. Nat. Cell Biol. *8*, 1114–1123.

Zhao, W., Ji, X., Zhang, F., Li, L., and Ma, L. (2012). Embryonic stem cell markers. Molecules *17*, 6196–6236.